

Risk-dependent centrality in economic and financial networks

Paolo Bartesaghi*, Michele Benzi†, Gian Paolo Clemente‡, Rosanna Grassi†, and Ernesto Estrada§

Abstract. Node centrality is one of the most important and widely used concepts in the study of complex networks. Here, we extend the paradigm of node centrality in financial and economic networks to consider the changes of node “importance” produced not only by the variation of the topology of the system but also as a consequence of the external levels of risk to which the network as a whole is submitted. Starting from the “Susceptible-Infected” (SI) model of epidemics and its relation to the communicability functions of networks we develop a series of risk-dependent centralities for nodes in (financial and economic) networks. We analyze here some of the most important mathematical properties of these risk-dependent centrality measures. In particular, we study the newly observed phenomenon of ranking interlacement, by means of which two entities may interlace their ranking positions in terms of risk in the network as a consequence of the change in the external conditions only, i.e., without any change in the topology. We test the risk-dependent centralities by studying two real-world systems: the network generated by collecting assets of the S&P 100 and the corporate board network of the US top companies, according to Forbes in 1999. We found that a high position in the ranking of the analyzed financial companies according to their risk-dependent centrality corresponds to companies more sensitive to the external market variations during the periods of crisis.

Key words. Communicability, Complex networks, SI models, Centrality measures, Risk propagation

AMS subject classifications. 05C82, 90B15, 91G80

1. Introduction. Modern economic and financial systems are characterized by a vast collection of interacting agents [2, 11, 47, 49, 54, 58, 65, 96]. In economic systems, for instance, the interdependence among entities characterizes the trade and exchange of goods in non-anonymous markets as well as in risk sharing agreements in developing countries [2]. In this framework, the agents’ interaction is responsible for the nature of the relations between the individual behavior and the aggregate behavior [65].

The human factor which underlies these economic and financial systems is also characterized by the interconnectivity. The existence of networks of interpersonal relations has been empirically observed to constitute a fundamental factor in shaping the inter-institution networks, or in accounting for the networks of risk-sharing agreements [29, 45, 46], the formation of buyer-seller networks [26, 52, 70], product adoption decisions [34, 64], diffusive processes [53, 57, 75], industrial organization [58], trade agreements [49] and even for the existence of interbank networks [2]. This is not surprising as humans are responsible for the execution of deals between the institutions to which they belong to [25, 69, 81].

*Department of Statistics and Quantitative Methods, University of Milano - Bicocca, Via Bicocca degli Arcimboldi 8, 20126, Milano, Italy (paolo.bartesaghi@unimib.it, rosanna.grassi@unimib.it).

†Scuola Normale Superiore, Piazza dei Cavalieri 7, 56126, Pisa, Italy (michele.benzi@sns.it).

‡Department of Mathematics for Economics, Financial and Actuarial Sciences, Università Cattolica del Sacro Cuore, Largo Gemelli 1, 20123, Milano (gianpaolo.clemente@unicatt.it).

§Institute of Mathematics and Applications (IUMA), Universidad de Zaragoza, Pedro Cerbuna 12, E-50009 Zaragoza, Spain; ARAID Foundation, Government of Aragon, 50018 Zaragoza, Spain (estrada66@unizar.es).

From a mathematical perspective all these interdependencies between economic and financial entities can be captured by the formal concept of network, in which nodes represent the entities (individuals, firms, countries, etc.) and edges account for the relations between such entities, ranging from social relations to trade agreements [41]. Hence, it is possible to use the tools of network theory to analyze the structure, the evolution and the dynamic processes that take place on these systems. On one side, researchers have studied the topological properties of these networks (sometimes called *static analysis*), which do not assume mechanisms of transmission of effects through the economic and financial entities [50, 62, 91]. Among such studies, it is frequent to find analyses of clusters formed by groups of institutions, as well as the centrality of individual nodes in the networks [13, 18, 88]. Specifically, centrality measures (see Chapter 5 in [41] for a detailed analysis) are topological characterizations of the nodes and their neighborhood in a network. In the analysis of financial and economic networks, the use of centrality measures is not so effective, as the classical ones provide a static view of the network and even other measures based on dynamic processes, such as random walks based centralities [80], do not capture the changing conditions to which these networks could be submitted in relatively short periods of time. As an illustrative example, let us consider a hypothetical interbank network for which we are interested in analyzing the risk-dependent exposure of the various entities of the system. Any centrality measure will point out a specific and static ranking of the nodes. However, a bank which is very central at a low-level of external risk is not necessarily central when such level of external risk increases, and vice versa. On the other hand, the propagation of shocks through these networks is considered and it is usually known as *dynamic analysis* [5, 24, 33, 38, 59]. In these studies, a specific way of transmission of these shocks through the network is assumed – as in the case of “Susceptible-Infected” and “Susceptible-Infected-Recovered” epidemiological models [73, 78, 85] – and then a systemic risk analysis is based on the contagion effects observed through such models.

In this work we develop a mathematical model to account for the risk exposure of an entity in a networked (economic or financial) system. This model is based on the relation between the Susceptible-Infected epidemiological model and the so-called communicability functions of a network [42]. Using this connection we derive new centrality indices that quantify the level of risk at which an entity is exposed to as a function of the global external level of risk. Our approach takes advantage of the benefits of both static and dynamic analyses. Indeed, unlike the standard approaches followed in the literature, these risk-dependent centralities are not static indices, as most of centrality indices are, but they vary with the change of the external global risk level at which the system is submitted to. More importantly, the ranking of the nodes in these networks also depends on this global external level of risk. This means that an entity – a node in the network – which is at low (high) level of risk under external conditions can be at high (low) level under different conditions.

We test our model by using two different systems, a network of assets based on the daily returns of the components of the S&P 100 for the period ranging from January 2001 to December of 2017 and a network representing the interconnection between companies in the US top corporates according to Forbes in 1999. In the first case we extract the essential information about asset correlations through the minimum spanning tree. We measure how the centrality of the assets changes at different values of the external risk. What emerges is a high volatility in the rankings during the financial crisis of 2007-2008, when the node centrality

proves to be more sensitive to the external risk. In the case of the corporate network we discuss, at first, the top companies according to their ranking in total communicability, both at low and at high risk, giving a possible explanation to its stability or its change. Then, we analyze a sample of significant companies, looking for a correlation between the shareholders value creation (SVC) and their behavior during and after the crisis period at which data were collected. We find that a remarkable increase in their risk-centrality ranking during a crisis corresponds to a less resilient reaction to the external market turmoil.

The paper is structured as follows. After a brief review of the literature (Subsection 1.1) and the necessary mathematical preliminaries (Section 2), we describe a Susceptible-Infected (SI) model on a financial network (Section 3) and we define the risk-dependent centrality proving some mathematical properties (Section 4). We perform numerical analyses of the proposed centrality for random networks (Section 5), then we apply the proposed measure to real-world financial networks (Sections 6 and 6.2) and we analyze the ranking interlacement problem (Section 7). Conclusions follow in Section 8.

1.1. Literature review. Global financial markets have increasingly been modeled and studied by means of network theory, as witnessed by the wide related literature. Networks are frequently considered meaningful in representing the structure of links between financial institutions, whether they are assets or liabilities (see, for instance, [2, 52, 96]). Such links can describe the exposures between banks acquired through the interbank market, in the first case, or can emerge when banks are connected through their liabilities, in the second one.

Networks are also a powerful tool in detecting how systemic risk rises and propagates through an interconnected banking system. Eisenberg and Noe [36] show the existence of a unique clearing vector as a consequence of an initial default of the system. This work inspired several authors that proposed applications and generalization of the Eisenberg and Noe model (see, for instance, [1] and [88]).

As summarized by Allen and Babus [2], most of the literature on financial and economic networks investigates how different network structures respond to the breakdown of a single institution in order to identify which ones are more fragile. Boss et al. [18] perform an empirical analysis on the Austrian banking system, analyzing the topological structure through different network measures, in order to assess how this structure affects the system stability with respect to the the default of a single bank.

In networked systems of any kind it is frequent to find contagion processes propagating effects from one node to another [85]. Economic and financial systems are not immune from such contagion processes due to their highly interconnected nature [3, 6, 19, 22, 28, 30, 37, 51, 55, 67, 73, 74, 92, 93]. In a seminal paper, Allen and Gale [3] show that the spread of contagion among banks depends on the interconnectedness patterns in the system. The contagion process seems to start from a given institution to its nearest neighbors first, which after collapsing propagate the shock in the form of a wave [48]. While this interconnectedness increases the chances of contagion, it is certainly responsible for absorbing the shocks, giving rise to the belief that financial and economic networks are “robust-yet-fragile” [20, 21, 50, 77, 92].

The impact of the topology on the stability of a financial system has been widely studied in order to describe the large-scale pattern of contagion processes inside the network [3, 73, 89]. The role of interconnectedness has been stressed: the more connected is the system,

the more easily counterpart losses of a failing institution can be dispersed to, and absorbed by, other entities inside the network [51]. The concept of “too-connected-to-fail” emerged alongside the “too-big-to-fail” paradigm [11, 92]. In this framework, several works exploited the relation between clustering coefficient and the level of financial distress in the market [17, 23, 79, 90]. Furthermore, it has been showed that networks with heterogeneous degree distributions are robust to random attacks but fragile to targeted attacks [19, 51]. Some authors focused on incomplete networks, revealing that they are more prone to contagion than complete structures. Better connected networks are more resilient since the proportion of the losses in one bank’s portfolio is transferred to more banks through interbank agreements [2, 62, 95]. Resilience measures, whose computation only involves the distribution of contagious links, have been proposed by [6, 31, 89]. The authors observe on a sample network that the size of the default cascade generated by a macroeconomic shock across balance sheets may exhibit a sharp transition when the magnitude of the shock reaches a certain threshold, beyond which the contagion spreads to a large fraction of the financial system. This domino effect (see [56, 12]) plays an important role in the real-world financial networks due to the growing interconnectedness between financial and economic institutions [89]. The role of non-adjacent nodes in contagion processes has been investigated in Susceptible-Infected-Recovered (SIR) models [30, 68, 72, 82]. Centrality of a given institution as best spreader node in a contagion process has been discussed by [73], who define the avalanche size of a given node as the number of subsequently collapsed institutions starting from a given institution’s collapse. In that way they are able to identify the most dangerous crisis epicenter of the network. The idea of best spreader node has also been studied in [94] in terms of topological centralities, which was previously investigated by Estrada and Hatano under the name of “vibrational centrality” [43].

Centralities have been also used as measures to assess contagion in the interbank market. In this framework, Dimitros and Vasileios [32] recommended the use of well-established centrality measures as a way to identify the most important variables in a network. Battiston et al. [13] introduce DebtRank, a centrality measure that accounts for distress in one or more banks, based on the possibility of losses occurring prior to default. From this work originates the concept that some banks might be too central to fail. The paper of Battiston et al. [13] has opened up a fruitful research line [7, 8, 9, 10].

2. Preliminaries. Here we use indistinctly the terms graphs and networks. Most of the network theoretic concepts defined hereafter can be found in [41]. A *simple graph* $\Gamma = (V, E)$ is defined by a set of n nodes (vertices) V and a set of m edges $E = \{(u, v) | u, v \in V\}$ between the nodes. The *degree* of a node, denoted by k_u , is the number of edges incident to u in Γ . The *adjacency matrix* of the graph $A = (A_{uv})_{n \times n}$ with entries $A_{uv} = 1$ if $(u, v) \in E$ or zero otherwise. We also consider here *weighted graphs* $\Gamma' = (V, E, W)$ in which $w_{uv} \in W$ is a positive number assigned to the corresponding edge $(u, v) \in E$. In this case the sum of the weights for all edges incident to a node is known as the *weighted degree* or *strength*. We consider here only undirected networks, such that $(u, v) \in E$ implies that $(v, u) \in E$. In this case the matrix A can be expressed as $A = U\Lambda U^T$ where $U = [\vec{\psi}_1 \cdots \vec{\psi}_n]$ is an orthogonal matrix of the eigenvectors of A and Λ is the diagonal matrix of eigenvalues $\lambda_1 \geq \lambda_2 \geq \cdots \geq \lambda_n$. The entries of $\vec{\psi}_j$ are denoted by $\psi_{j,1}, \dots, \psi_{j,n}$.

An important quantity for studying communication processes in networks is the communicability function [42], defined for a pair of nodes u and v as

$$G_{uv} = \sum_{k=0}^{\infty} \frac{(A^k)_{uv}}{k!} = (\exp(A))_{uv} = \sum_{j=1}^n e^{\lambda_j} \psi_{j,u} \psi_{j,v}.$$

It counts the total number of walks starting at node u and ending at node v , weighted in decreasing order of their length by a factor of $\frac{1}{k!}$. A *walk* of length k in Γ is a set of nodes $i_1, i_2, \dots, i_k, i_{k+1}$ such that for all $1 \leq l \leq k$, $(i_l, i_{l+1}) \in E$. A *closed walk* is a walk for which $i_1 = i_{k+1}$. Therefore, G_{uv} is considering shorter walks as more influential than longer ones. The matrix exponential is an example of a general class of matrix functions which are expressible as

$$(2.1) \quad (f(A))_{uv} = \sum_{k=0}^{\infty} c_k (A^k)_{uv},$$

where c_k are coefficients giving more weight to the shorter than to the longer walks, and making the series converge. The term G_{uu} , which counts the number of closed walks starting at the node u giving more weight to the shorter than to the longer ones, is known as the subgraph centrality of the node u .

We also consider here a Susceptible-Infected (SI) model on the nodes and edges of the network. In this case a node can be susceptible and then get infected from a nearest neighbor or it is infected and can transmit the infection to other susceptible nodes. Let γ be the infection rate *per link*. Let $X_i(t)$ be a random variable on node i such that

$$(2.2) \quad X_i(t) = \begin{cases} 1 & \text{if node } i \text{ is infected at time } t \\ 0 & \text{if node } i \text{ is healthy at time } t. \end{cases}$$

Then we define

$$(2.3) \quad x_i(t) = P[X_i(t) = 1] = \mathbb{E}[X_i(t)] \in [0, 1],$$

which is the probability that node i is infected at time t . For the whole network, we define the vector of probabilities:

$$(2.4) \quad \vec{x}(t) = [x_1(t), \dots, x_n(t)]^T.$$

3. Model. Let us consider a SI model on a financial network. That is the nodes of a graph $\Gamma = (V, E)$ represent financial institutions and the edges connecting them represent an interaction that can transmit a “disease” from one institution to another. A node can be susceptible and then get infected from a nearest neighbor or it is infected and can transmit

the infection to other susceptible nodes. Let γ be the infection rate and let $x_i(t)$ be the probability that node i get infected at time t from any infected nearest neighbor. Then,

$$(3.1) \quad \frac{dx_i(t)}{dt} = \vec{x}(t) = \gamma(1 - x_i(t)) \sum_{j=1}^n A_{ij}x_j(t), \quad t \geq t_0,$$

which in matrix-vector form becomes:

$$(3.2) \quad \dot{\vec{x}}(t) = \gamma[1 - \text{diag}(\vec{x}(t))] A \vec{x}(t),$$

with initial condition $\vec{x}(0) = \vec{x}_0$.

It is well-known that on a strongly connected network [78]:

1. if $\vec{x}_0 \in [0, 1]^n$ then $\vec{x}(t) \in [0, 1]^n$ for all $t > 0$;
2. $\vec{x}(t)$ is monotonically non-decreasing in t ;
3. there are two equilibrium points: $\vec{x}^* = \vec{0}$, i.e. no epidemic, and $\vec{x}^* = \vec{1}$ (the vector of all ones), i.e., full contagion;
4. the linearization of the model around the point $\vec{0}$ is given by

$$(3.3) \quad \dot{\vec{x}}(t) = \gamma A \vec{x}(t)$$

and it is exponentially unstable;

5. each trajectory with $\vec{x}_0 \neq \vec{0}$ converges asymptotically to $\vec{x}^* = \vec{1}$, i.e. the epidemic spreads monotonically to the entire network.

In particular, the linearized problem comes from the following observation. It can be checked that

$$(3.4) \quad \dot{x}_i(t) = \gamma[1 - x_i(t)] \sum_{j=1}^n A_{ij}x_j(t) \leq \gamma \sum_{j=1}^n A_{ij}x_j(t)$$

or

$$(3.5) \quad \dot{\vec{x}}(t) \leq \gamma A \vec{x}(t),$$

$\forall i$ and $\forall t$. Then, we can use the linear dynamical system

$$(3.6) \quad \dot{\vec{x}}(t) = \gamma A \vec{x}(t)$$

as an upper-bound for the original non-linear dynamical system.

A solution for the linearized problem can be written as

$$(3.7) \quad \vec{x}(t) = e^{\gamma t A} \vec{x}_0,$$

which using the spectral decomposition of A can be written as

$$(3.8) \quad \vec{x}(t) = \sum_{j=1}^n e^{\gamma t \lambda_j} \vec{\psi}_j \vec{\psi}_j^T \vec{x}_0.$$

This solution to the linearized model is affected by the following main problems:

1. $\vec{x}(t)$ grows quickly without bound, in spite of the fact that $\vec{x}(t)$ is a vector of probabilities which should not exceed the unit;
2. $\vec{x}(t)$ is an accurate solution to the nonlinear SI problem only if $t \rightarrow 0$ and $\vec{x}_0 \rightarrow 0$.

In order to sort out these difficulties we follow a recent work by Lee et al. [72] and introduce the following new variable

$$(3.9) \quad y_i(t) := -\log(1 - x_i(t)),$$

which is an increasing convex function. Then, as $1 - x_i$ is the probability that node i is not infected at a given time, the new variable $y_i(t)$ represents the information content or surprise of the node i of being infected (see, e.g., [27]). We can now write down the SI model (3.1) as

$$(3.10) \quad \frac{dy_i(t)}{dt} = \dot{y}_i(t) = \gamma \sum_{j=1}^n A_{ij} x_j(t), \quad t \geq t_0,$$

or

$$(3.11) \quad \vec{y}(t) = \gamma A \vec{x}(t).$$

The complete solution to the SI model is then given by

$$(3.12) \quad \vec{x}(t) = \vec{1} - e^{-\vec{y}(t)},$$

where $e^{-\vec{y}(t)}$ is the vector in which the i th entry is $e^{-y_i(t)}$ and

$$(3.13) \quad \begin{aligned} \vec{y}(t) = & e^{\gamma t A \text{diag}(\vec{1} - \vec{x}_0)} [-\log(1 - \vec{x}_0)] \\ & + \sum_{j=0}^{\infty} \frac{(\gamma t)^{j+1}}{(j+1)!} \left[A \text{diag}(\vec{1} - \vec{x}_0) \right]^j A \left(\vec{x}_0 + (\vec{1} - \vec{x}_0) \log(\vec{1} - \vec{x}_0) \right). \end{aligned}$$

From a practical point of view, the interesting case of the dynamics is when $\vec{x}_0 < \vec{1}$, in which case the solution simplifies to

$$(3.14) \quad \vec{y}(t) = \vec{y}_0 + \left[e^{\gamma t A \text{diag}(\vec{1} - \vec{x}_0)} - I \right] \cdot \text{diag}(\vec{1} - \vec{x}_0)^{-1} \vec{x}_0.$$

As we can see, the matrix A is replaced by the matrix $W = A \text{diag}(\vec{1} - \vec{x}_0)$, which is equivalent to a weighted adjacency matrix with entries $w_{ij} = A_{ij}(1 - x_{0j})$. Now, we can make the assumption that the initial probabilities of being infected are equal for every node, i.e. that at the beginning every node has the same probability p to be infected and to be the one from which the epidemic starts. This means that we are asking for

$$(3.15) \quad x_{0i} = p = \frac{c}{n}, \quad \forall i = 1, \dots, n$$

for some scalar constant c . In this case $\text{diag}(\vec{1} - \vec{x}_0) = (1 - \frac{c}{n})I = (1 - p)I$. If we set $\alpha = 1 - p$, the solution of the SI on the network becomes:

$$(3.16) \quad \vec{y}(t) = \vec{y}_0 + \frac{1 - \alpha}{\alpha} [e^{\alpha \gamma t A} - I] \vec{1}.$$

and since $\vec{y}_0 = (-\log \alpha) \vec{1}$,

$$(3.17) \quad \vec{y}(t) = \left(\frac{1}{\alpha} - 1\right) e^{\alpha \gamma t A} \vec{1} - \left(\log \alpha + \frac{1 - \alpha}{\alpha}\right) \vec{1}.$$

Finally, componentwise, we get

$$(3.18) \quad y_i(t) = \left(\frac{1}{\alpha} - 1\right) \mathcal{R}_i - \left(\log \alpha + \frac{1 - \alpha}{\alpha}\right),$$

where \mathcal{R}_i is the total communicability of the node i . Keeping in mind that $-\log \alpha = y_i(0)$ and $\alpha = 1 - p$, we can write the previous equation also as

$$(3.19) \quad \Delta y_i(t) = y_i(t) - y_i(0) = \left(\frac{p}{1 - p}\right) (\mathcal{R}_i - 1),$$

which means that $\mathcal{R}_i - 1$ at time t is proportional to the variation in the information content of node i from time 0 to time t . Finally, the probability of node i of being infected at time t can be expressed in terms of \mathcal{R}_i as

$$(3.20) \quad x_i(t) = 1 - (1 - p)e^{-\frac{p}{1-p}(\mathcal{R}_i - 1)}.$$

When the parameter c is fixed, the number of infected nodes depends only on the term $e^{\gamma t A} \vec{1}$. Let us consider the time evolution of an infection in an Erdős-Rnyi network with 100 nodes and 400 edges. The results are illustrated in [Figure 1](#) for two different values of the infectivity rate.

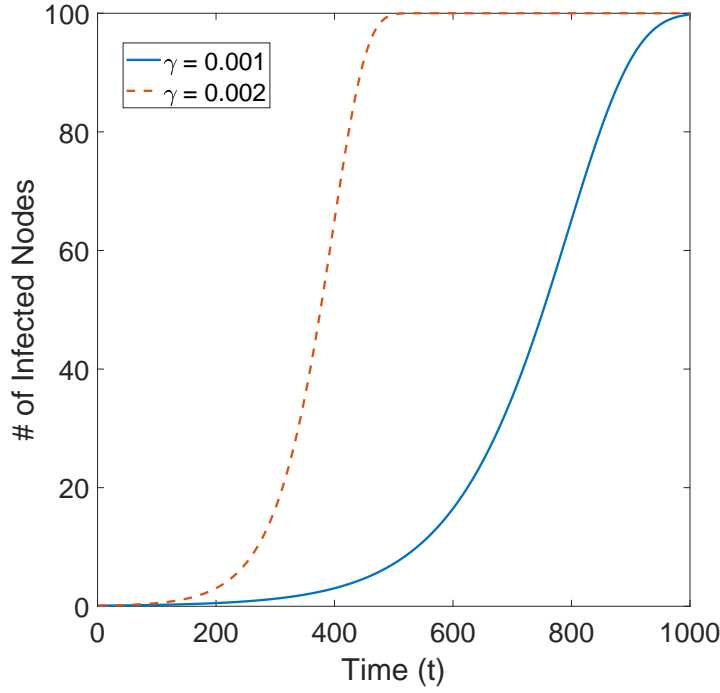


Figure 1: Simulation of the progression of a SI epidemics on an Erdős-Rényi network with 100 nodes and 400 edges. The parameters used in the modeling are $c = 0.001$ and two different values of the infectivity parameter γ as indicated in the plot.

4. Risk-dependent centrality. Let us designate $\zeta = \alpha\gamma$, which determines the level of risk to which the whole network is submitted. For instance, for $\zeta = 0$ there is no risk of infection on the network as a node cannot transmit the disease to a nearest neighbor. This situation corresponds to the case of isolated nodes (no edges). When $\zeta \rightarrow \infty$ the risk of infection is very high due to the fact that for a fixed value of c the infectivity is infinite. Therefore, we call $\mathcal{R}_i = \left(e^{\zeta A} \vec{1}\right)_i$ the risk-dependent centrality of the node i . That is, the values of \mathcal{R}_i reflects how central a node is in “developing” the epidemics on the network. As the networks considered are undirected, this centrality accounts for both the facility with which the node gets infected as well as the propensity of this node to infect other nodes. The index \mathcal{R}_i can be expressed as

$$(4.1) \quad \mathcal{R}_i = \left(\left(I + \zeta A + \zeta^2 \frac{A^2}{2!} + \zeta^3 \frac{A^3}{3!} + \dots \right) \vec{1} \right)_i,$$

which indicates that it counts the number of walks of different lengths, that have started at the corresponding node, weighted by a factor $\frac{\zeta^k}{k!}$. It is straightforward to realize from the definition of the risk-dependent centrality that it can be split into two contributions. That is, \mathcal{R}_i is composed by a weighted sum of all closed walks that start and end at i , $(e^{\zeta A})_{ii}$ and by the weighted sum of walks that start at the node i and end elsewhere, $\sum_{j \neq i} (e^{\zeta A})_{ij}$

$$(4.2) \quad \mathcal{R}_i = \left(e^{\zeta A}\right)_{ii} + \sum_{j \neq i} \left(e^{\zeta A}\right)_{ij} := \mathcal{C}_i + \mathcal{T}_i,$$

where the first term in the right-hand side represents the circulability of the disease around a given node and the second one represents the transmissibility of the disease from the given node to any other in the network. The circulability is very important because it accounts for the ways the disease has to become endemic. For instance, a large circulability for a node i implies that the disease can infect its nearest neighbors and will keep coming back to i over and over again in a circular way. We start now by proving some results about these risk-dependent centralities. The following theorem is a special case of results found, for instance, in [16].

Theorem 4.1. *The node degree k_i and the eigenvector centrality are limiting cases of the risk-dependent centrality \mathcal{R}_i when the external level of risk ζ on the network is low or high, respectively.*

Proof. We begin by observing that the ranking of nodes, in terms of their risk-dependent centrality, is unaffected if all the centralities \mathcal{R}_i are shifted and rescaled by the same amount. That is, the same ranking is obtained using either \mathcal{R}_i or the equivalent measure

$$\hat{\mathcal{R}}_i = \frac{\mathcal{R}_i - 1}{\zeta},$$

where $\zeta > 0$. Now, we have

$$(4.3) \quad \hat{\mathcal{R}}_i = \left[\left(A + \frac{\zeta}{2!} A^2 + \dots \right) \vec{1} \right]_i = k_i + \frac{\zeta}{2!} (A^2 \vec{1})_i + O(\zeta^2).$$

Hence, in the limit of $\zeta \rightarrow 0$, the ranking given by \mathcal{R}_i is identical to degree ranking.

To study the limit for ζ large we write

$$(4.4) \quad \mathcal{R}_i = \left[e^{\zeta A} \vec{1} \right]_i = \sum_{k=1}^n e^{\zeta \lambda_k} (\psi_k^T \vec{1}) \psi_{k,i} = e^{\zeta \lambda_1} (\psi_1^T \vec{1}) \psi_{1,i} + \sum_{k=2}^n e^{\zeta \lambda_k} (\psi_k^T \vec{1}) \psi_{k,i}.$$

We note again that for ranking purposes we can use the equivalent measure obtained by dividing all risk-dependent centralities by the same quantity, $e^{\zeta \lambda_1} (\psi_1^T \vec{1})$, which is strictly positive. That is, we can use

$$(4.5) \quad \tilde{\mathcal{R}}_i = \psi_{1,i} + \frac{1}{\psi_1^T \vec{1}} \sum_{k=2}^n e^{\zeta (\lambda_k - \lambda_1)} (\psi_k^T \vec{1}) \psi_{k,i}.$$

Since the network is connected, the Perron–Frobenius Theorem insures that $\lambda_1 > \lambda_2 \geq \dots \geq \lambda_n$. Hence, each term $e^{\zeta (\lambda_k - \lambda_1)}$ for $k = 2, \dots, n$ vanishes in the limit as $\zeta \rightarrow \infty$, and we see from (4.5) that the risk-dependent centrality measure gives the same ranking as eigenvector centrality for ζ large. ■

It is interesting to observe that the risk-dependent centrality of every node also depends on the (strictly positive) quantity

$$\psi_1^T \vec{1} = \sum_{j=1}^n \psi_{1,j},$$

see Equation (4.4). The larger this quantity is, the higher is the risk-dependent centrality of each node. Assuming that the dominant eigenvector is normalized so as to have Euclidean norm equal to 1, it is well known that this quantity is always between 1 and \sqrt{n} . The value 1 is never attained for a connected graph. It can only be approached in the limit as all the eigenvector centrality is concentrated on one node, say node i , where it takes values arbitrarily close to 1, with the values $\psi_{1,j}$ for all $j \neq i$ taking arbitrarily small values. An example of this would be the star graph S_n for $n \rightarrow \infty$. The maximum value is attained in the case where all nodes have the same eigenvector centrality: $\psi_{1,1} = \psi_{1,2} = \dots = \psi_{1,n}$ (i.e., in the case of regular graphs).

Let us return to the decomposition $\mathcal{R}_i = \mathcal{C}_i + \mathcal{T}_i$ of the risk-dependent centrality of a node into its two components, circulability and transmissibility. Similar considerations apply to these quantities. We summarize them in the following result.

Theorem 4.2. *The node degree k_i and the eigenvector centrality are limiting cases of the risk-dependent circulability \mathcal{C}_i when the external level of risk ζ on the network is low or high, respectively. The same is true for the risk dependent transmissibility.*

Proof. The proof for the circulability is a straightforward adaptation of that for the total communicability; see also [16].

We give the details for the transmissibility, which has not been analyzed before. We have for $i \neq j$ that

$$\left(e^{\zeta A}\right)_{ij} = \zeta A_{ij} + \frac{\zeta^2}{2!} w_{i,j}^{(2)} + O(\zeta^3),$$

where $w_{i,j}^{(2)}$ denotes the number of walks of length two between node i and node j . Dividing by $\zeta > 0$, summing over all $j \neq i$ and taking the limit as $\zeta \rightarrow 0$, we find

$$\zeta^{-1} \mathcal{T}_i = \zeta^{-1} \sum_{j \neq i} \left(e^{\zeta A}\right)_{ij} \rightarrow \sum_{j \neq i} A_{ij} = k_i,$$

where we have used the fact that $A_{ii} = 0$, for all i . Hence, transmissibility is equivalent to node degree in the small ζ limit. For the large ζ limit we write

$$\mathcal{T}_i = \sum_{j \neq i} \sum_{k=1}^n e^{\zeta \lambda_k} \psi_{k,i} \psi_{k,j} = e^{\zeta \lambda_1} \psi_{1,i} \sum_{j \neq i} \psi_{1,j} + \sum_{k=2}^n e^{\zeta \lambda_k} \left[\sum_{j \neq i} \psi_{k,i} \psi_{k,j} \right].$$

Dividing by the positive constant $e^{\zeta \lambda_1} \sum_{j \neq i} \psi_{1,j}$ and taking the limit as $\zeta \rightarrow \infty$, the second part of the right-hand side vanishes and we obtain again the eigenvector centrality $\psi_{1,i}$ of node i . ■

We conclude this section with some remarks on the various measures \mathcal{R}_i , \mathcal{C}_i and \mathcal{T}_i . While they all display the same limiting behavior and provide identical rankings in the small and

large ζ limits, they provide different insights on the network structure (and therefore on node risk). For instance, it is well known that subgraph centrality (which is the same as circulability, see [44, 41]) can discriminate between the nodes of certain regular graphs, that is, graphs in which all the nodes have the same degree. The same holds for transmissibility. Total communicability, on the other hand, is unable to discriminate between the nodes of regular graphs (and neither are degree and eigenvector centrality, of course). These measures are also different from a computational viewpoint. One advantage of the risk centrality based on total communicability is that it only requires the computation of the action of the matrix exponential $e^{\zeta A}$ on the vector $\vec{1}$. The entries of the resulting vector can be computed efficiently without having to compute any entry of $e^{\zeta A}$, see [15]. Modern Krylov-type iterative methods (like those based on the Lanczos or Arnoldi process) can handle huge networks (with many millions of nodes) without any difficulty. In contrast, the computation of the circulability requires the explicit computation of the diagonal entries of $e^{\zeta A}$ (the node transmissibility is then easily obtained by subtracting the circulability from the total communicability). Although there are techniques that can handle fairly large graphs (see [14]), these calculations are much more expensive than those for the total communicability. This limits the size of the networks that they can be applied to. However, for most financial networks the computation of the circulability is still feasible.

5. Numerical Analysis. In this section we carry out extensive centrality computations for a variety of networks, with the aim of analyzing the behavior of circulability, transmissibility and risk-dependent centrality for different values of ζ . We initially compute them for simulated graphs generated by using the Erdős-Rnyi (ER) model $\Gamma_{ER}(n; m)$ (see [40, 39]) with n vertices and m links and where each link is included with a probability independent from every other link. Graphs have been derived randomly and by ensuring that they are connected. Here we discard simulations where the obtained graph is not connected.

In particular, in order to test how the graph density affects the results, we have generated 17 $\Gamma_{ER}(n; m)$ graphs with $n = 100$ and varying the number of edges m . We report in Figure 2 the behavior of risk-dependent centrality and circulability, computed assuming $\zeta = 1$. Since the values of \mathcal{R}_i are significantly increasing when the density of the graph increases, we display in Figure 2(a), the distributions of the ratio between the risk-dependent centrality of each node \mathcal{R}_i and the average risk-dependent centrality. As might be expected, the centralities of nodes tend to be similar when we move towards the complete graph (i.e. we observe a lower variability of the distribution of ratios). Similar behaviors are also observed for \mathcal{C}_i and \mathcal{T}_i , with an higher volatility for the circulability (see Figure 2(b) and Figure 2(c)).

In Figure 2(d), we show the distributions of the incidence of the circulability \mathcal{C}_i on the risk-dependent centrality \mathcal{R}_i . When $\zeta = 1$, for all the graphs analyzed, the median value is around $\frac{1}{n}$, implying that the transmissibility has a median incidence of $\frac{n-1}{n}$ on \mathcal{R}_i . Also in this case, it is noteworthy to look at the variability of the distributions. When density is extremely low (i.e. very sparse graphs are considered), the heterogeneity of the nodes degree affects the ratio $\frac{\mathcal{C}_i}{\mathcal{R}_i}$. For instance, when the density is equal to 0.1, the circulability of a node ranges approximately from 0.2% to 1.8% of the risk-dependent centrality of the same node. In this case, the maximum and minimum ratios $\frac{\mathcal{C}_i}{\mathcal{R}_i}$ are attained by the nodes with the maximum and minimum degree, respectively.

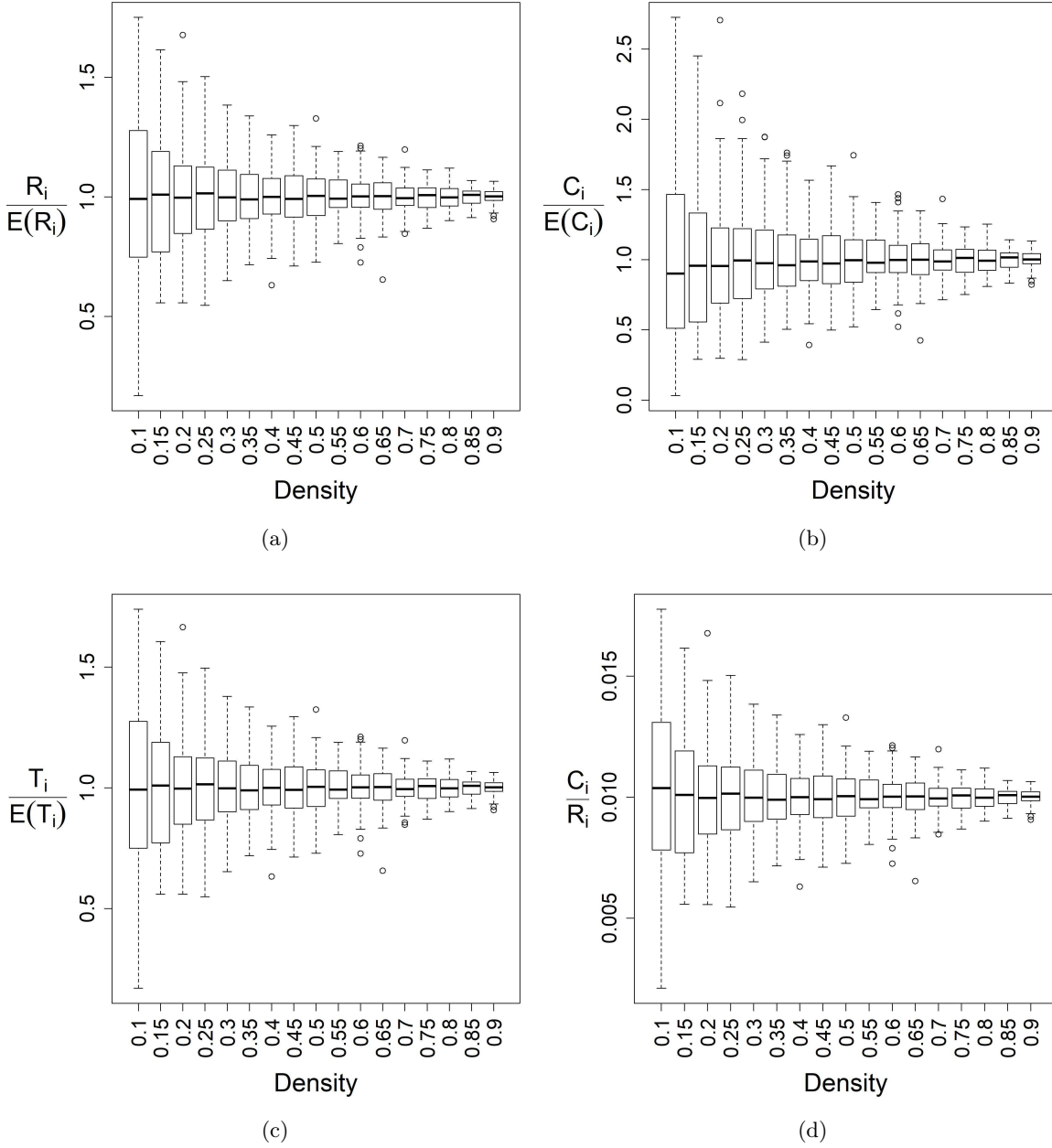


Figure 2: Figure a) displays the distributions of the ratios between the risk-dependent centrality of each node \mathcal{R}_i and the average risk-dependent centrality $E(\mathcal{R}_i)$, computed assuming $\zeta = 1$. Figure b) and c) display the analogous distributions for circulability and transmissibility. Figure d) shows the distributions of the ratios between the circulability \mathcal{C}_i and the risk-dependent centrality of each node \mathcal{R}_i , computed assuming $\zeta = 1$. All Figures are based on 17 graphs, generated by a $\Gamma_{ER}(100; m)$ model with a density varying between 0.1 and 0.9.

Next, we explore the effect of the risk of infections ζ on the nodes (see Figure 3). Focusing on the risk-dependent centrality ratio $\frac{\mathcal{R}_i}{E(\mathcal{R}_i)}$, we observe that the standard deviation between nodes is lower in a low-risk framework ($\zeta = 0.1$) than in a high-risk one ($\zeta = 2$). For instance, when the density is equal to 0.1, the standard deviation of the ratio moves from 0.18 for $\zeta = 0.1$ to 0.28 and 0.30 for ζ equal to 1 and 2, respectively. This behavior can be justified by the fact that differences between nodes tend to be enhanced when the network is highly risk-exposed. As already noticed, when the density increases, the node's behavior tends to be similar. In particular, we observe a correlation, between the risk-dependent centralities, for the lowest and the highest values of ζ , higher than 0.99 for ER graphs with a density greater than 0.15.

Furthermore, the pattern of $\frac{\mathcal{C}_i}{E(\mathcal{C}_i)}$ for low values of ζ is very peculiar. In this case, when the network is very sparse, nodes show a similar circulability, while higher differences are observed when the density is around 0.5.

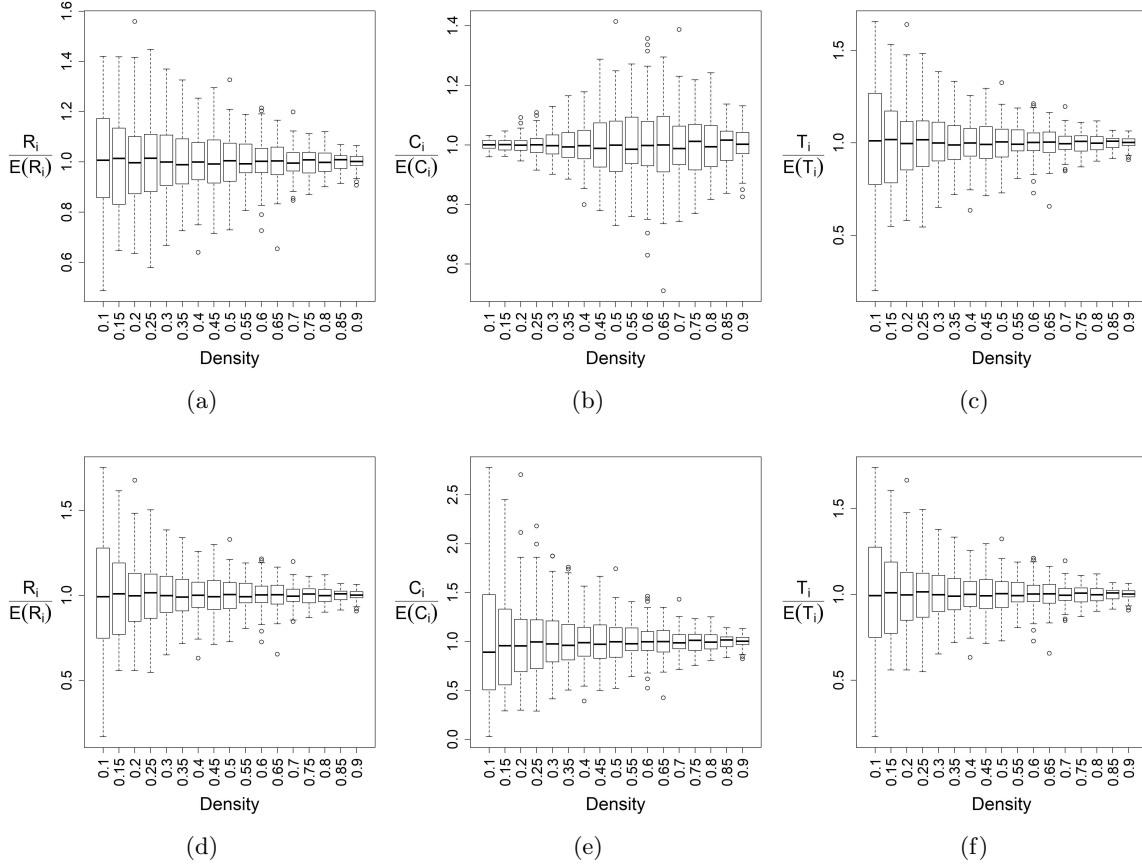


Figure 3: Figures a), b) and c) display the distributions of ratios $\frac{\mathcal{R}_i}{E(\mathcal{R}_i)}$, $\frac{\mathcal{C}_i}{E(\mathcal{C}_i)}$ and $\frac{\mathcal{T}_i}{E(\mathcal{T}_i)}$, respectively, computed in case of a low external risk ($\zeta = 0.1$). Figures d), e), f) show the distributions of the same ratios for an higher external risk ($\zeta = 2$).

In Figure 4, we report the incidence of the circulability on the risk-dependent centrality for different nodes and in case of different levels of risk ζ . In case of sparse networks (left-side in Figure 4), when the external risk is low, we have that the infection remains in larger part circulating in a loopy way around the nodes, while only a lower proportion of risk tends to be transmitted to other nodes. This is because for A sparse and ζ small, the matrix $e^{\zeta A} = I + \zeta A + \frac{\zeta^2}{2} A^2 + O(\zeta^3)$ is strongly diagonally dominant. In the case of $\zeta = 1$, as already observed, we have an average incidence of the circulability \mathcal{C}_i around $\frac{1}{n}$. A higher risk leads to a further reduction of the ratio. On the contrary, when a very dense network is considered, the ratio $\frac{\mathcal{C}_i}{\mathcal{R}_i}$ is very little affected by the external risk. In this case, both \mathcal{C}_i and \mathcal{R}_i increase at the same rate when ζ increases.

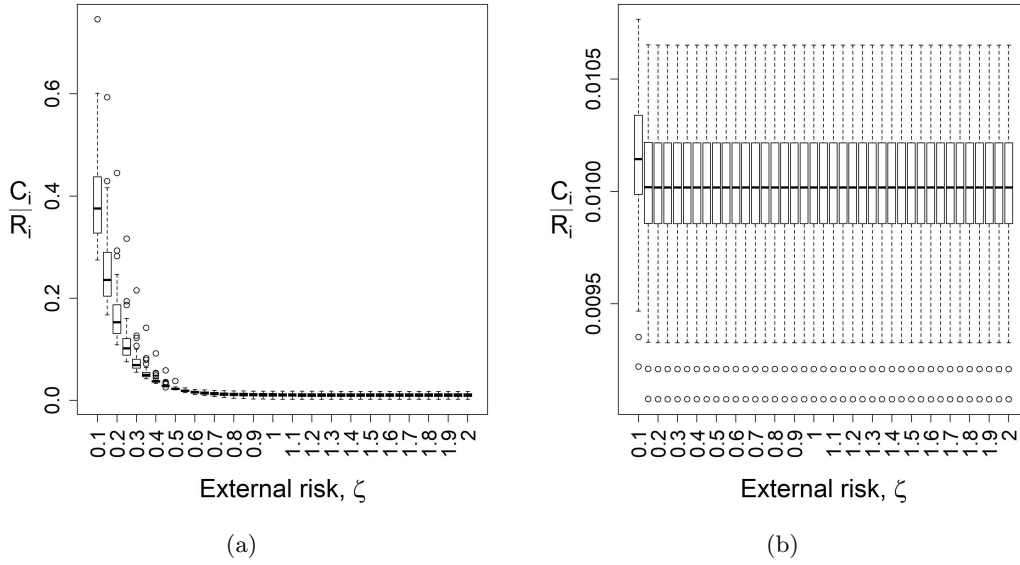


Figure 4: Figures report the distribution of the ratios between the circulability \mathcal{C}_i and the risk-dependent centrality of each node \mathcal{R}_i , computed for different ζ and by using generated ER graphs with a density equal to 0.1 (Figure a) and 0.9 (Figure b), respectively.

Next, we focus on the similarities in the rankings. In particular, we are interested in determining if, or for what type of networks, the different centrality measures provide similar rankings. To this end, we display in Table 1 the Spearman's rank correlation coefficient between the risk dependent centrality and the circulability for different graph densities and for various values of ζ . On average, we observe a strong positive monotonic dependence between the two centrality measures. As expected, the two measures tend towards the perfect monotonicity as the density arises. It is noteworthy the behavior with respect to ζ . The higher dependence is observed in a low-risk framework ($\zeta = 0.1$), while a slight reduction is noticeable when higher risk contexts are analyzed, providing again an empirical evidence of the fact that differences between nodes are increased in stressed conditions. Furthermore, this result is in line with the higher incidence of \mathcal{C}_i on \mathcal{R}_i as ζ vanishes. For the sake of brevity,

we do not report the Spearman correlation between \mathcal{R}_i and \mathcal{T}_i . However, in all cases, the coefficient is larger than 0.9999.

Table 1: Spearman’s rank correlation coefficients between \mathcal{C}_i and \mathcal{R}_i in ER graphs with 100 vertices and different densities. Correlations have been computed for different values of ζ .

| | | Density | | | | |
|---------|-----|---------|--------|--------|--------|--------|
| | | 0.1 | 0.3 | 0.5 | 0.7 | 0.9 |
| ζ | 0.1 | 0.9947 | 0.9967 | 0.9971 | 0.9994 | 0.9998 |
| | 0.5 | 0.9844 | 0.9950 | 0.9966 | 0.9994 | 0.9998 |
| | 1.0 | 0.9813 | 0.9950 | 0.9966 | 0.9994 | 0.9998 |
| | 1.5 | 0.9809 | 0.9950 | 0.9966 | 0.9994 | 0.9998 |
| | 2.0 | 0.9809 | 0.9950 | 0.9966 | 0.9994 | 0.9998 |

6. Analysis of real-world financial networks. In this section, we perform some empirical studies in order to assess the effectiveness of the proposed approaches. We consider two different networks. In the first we collected daily returns of a dataset referred to the time-period ranging from January 2001 to December 2017, that includes 102 leading U.S. stocks constituents of the *S&P* 100 index at the end of 2017. Data have been downloaded from Bloomberg. Returns have been split by using monthly stepped six-months windows. It means that the data of the first in-sample window of width six-month are used to build the first network. The process is repeated rolling the window one month forward until the end of the dataset is reached, obtaining a total of 199 networks. The first network, denoted as “1-2001” covers the period 1st of January 2001 to 30th of June 2001. The latter one (“7-2017”) covers the period 1st of July 2017 to 31th of December 2017.

Hence, for each window, we have a network $\Gamma_t = (V_t, E_t)$ (with $t = 1, \dots, 199$), where assets are nodes and links are weighted by computing the correlation coefficient ${}_t\rho_{i,j}$ between the empirical returns of each couple of assets. Notice that the number of assets can vary over time. Indeed, as mentioned, we have considered the 102 assets constituents of the *S&P* 100 index at the end of 2017. Some of these assets have no information available for some specific time periods. Therefore, in each window, we have considered only assets, whose observations are sufficiently large to assure a significant estimation of the correlation coefficient. However, it is not the aim of this paper to deal with the effects of alternative estimation methods. As a consequence, the number of nodes in the 199 networks varies from 83 to 102 during the time-period.

Then, we follow the methodology proposed in [76, 83] and we use the non-linear transformation, based on distances ${}_td_{i,j}$: ${}_td_{i,j} = \sqrt{2(1 - {}_t\rho_{i,j})}$. The distance matrix $D_t = [{}_td_{i,j}]_{i,j \in V_t}$, with elements $0 \leq {}_td_{i,j} \leq 2$, becomes the weighted adjacency matrix of the graph Γ_t . As proposed in [83], we extract the minimum spanning tree T_t . This is a simple connected graph that connects all n_t nodes of the graph with $n_t - 1$ edges such that the sum of all edge weights $\sum_{{}_td_{i,j} \in T_t} {}_td_{i,j}$ is minimum. As shown in [83], this minimum spanning tree, as a strongly reduced representative of the whole correlation matrix, bears the essential information about

asset correlations. Furthermore, the study of the centrality of nodes and the analysis of the evolution of the tree over time are two critical issues in portfolio selection problem (see [83, 86, 87]).

The second dataset consists of a network of the top corporates in US in 1999 according to Forbes magazine. The network is constructed as follows. First we consider a bipartite network in which one set of nodes consists of companies and the other of Chief Executive Officer (CEO)'s of such companies. As one CEO can be in more than one company we make a projection of this bipartite graph into the company-company space. In this way, the nodes represent corporations and two corporations are joined by an edge if they share at least one director. We consider two versions of this network, in the first we use the number of directors shared by two companies as an edge weight, and in the second we use the binary version of the first. We will refer to these as to the weighted and binary network, respectively. The network has 824 nodes, made up of one giant component of 814 nodes. We selected the giant component, with its binary and weighted adjacency matrices.

Networks, derived by both datasets, have been studied by computing the total communicability, circulability and transmissibility for each node with ζ varying in $(0, 1]$ with step 0.01.

6.1. Network of assets. Starting from the asset trees T_t , we measure the relevance of each node by using the risk-dependent centrality \mathcal{R}_i and by testing different values of ζ . We consider in Figure 5 the rankings' distribution of each asset. Different outcomes of each distribution have been obtained by computing the rankings based on \mathcal{R}_i for alternative values of ζ in the interval $(0; 1]$ with step 0.01. These results regard the first network "1-2001", namely, the network based on data that cover the period 1st of January 2001 to 30th of June 2001. We observe that some nodes show a significant variability according to different values of ζ . Indeed, some assets have climbed more than 20 positions in the ranking when ζ increases. For instance, Amazon (node 7 in Figure 5) moved from position 66 to 41 in case of low and high risk, respectively. Vice versa, Exelon Group (node 32 in Figure 5) lowered its ranking from 15 to 46. On the other hand, the most central nodes in the network remain very central also when external risk is very high. We have indeed that the top 6 is quite stable for different values of ζ . Top assets only exchange a bit their position, preserving their central role. For instance, United Technologies Corporation (node number 79 in Figure 5) is at the top of the ranking, independent of ζ .

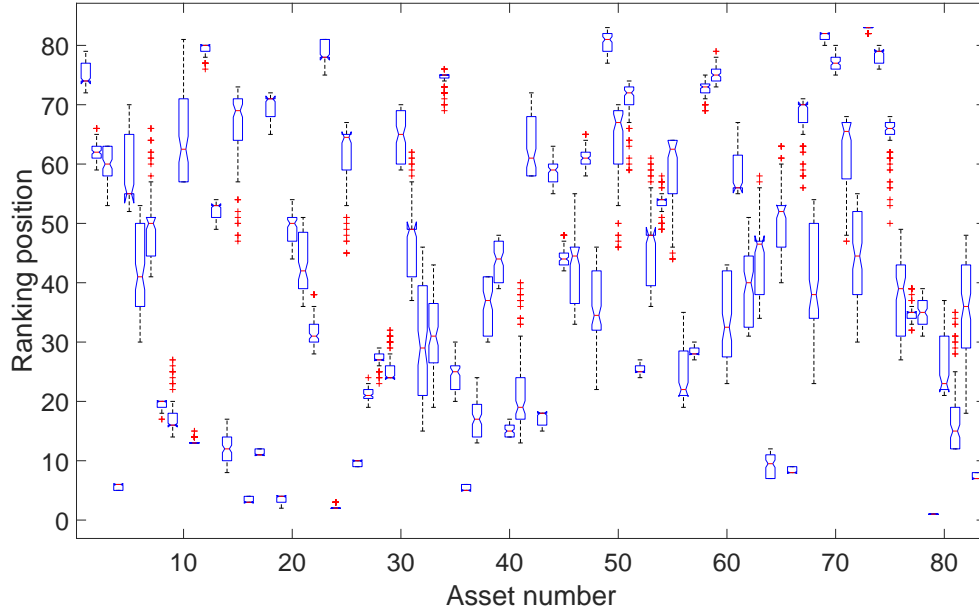


Figure 5: Figure reports the distribution of nodes' rankings based on \mathcal{R}_i with respect to ζ . For each distribution, the set of outcomes is given by the rankings of \mathcal{R}_i computed for alternative values of ζ . Results regard the network T_1 , i.e. the asset-tree in the first window 1 – 2001.

If we consider the period of the global financial crisis of 2007-2008 (see Figure 6 and 7), we observe an increase in the rankings' volatility. In shock periods, centrality of nodes is more affected by the value of ζ . We observe, for instance, that some assets move down by approximately 60 positions from a low risk to an high risk framework. Two examples are represented by Danaher Corporation and Honeywell International (assets 28 and 43, respectively, in Figure 6). Instead, Accenture PLC (node 3 in Figure 6) increased its ranking from position 61 to 11.

Even top central nodes are affected by ζ as the volatilities of their rankings show. It is instead confirmed the relevance of United Technologies Corporation (node number 82 in Figure 6 and 83 in Figure 7) that is again at the top of the ranking at the end of 2017, independent of ζ . At the end of 2008, the centrality of this asset is also confirmed, although, a bit of variability in the ranking is observed for this firm.

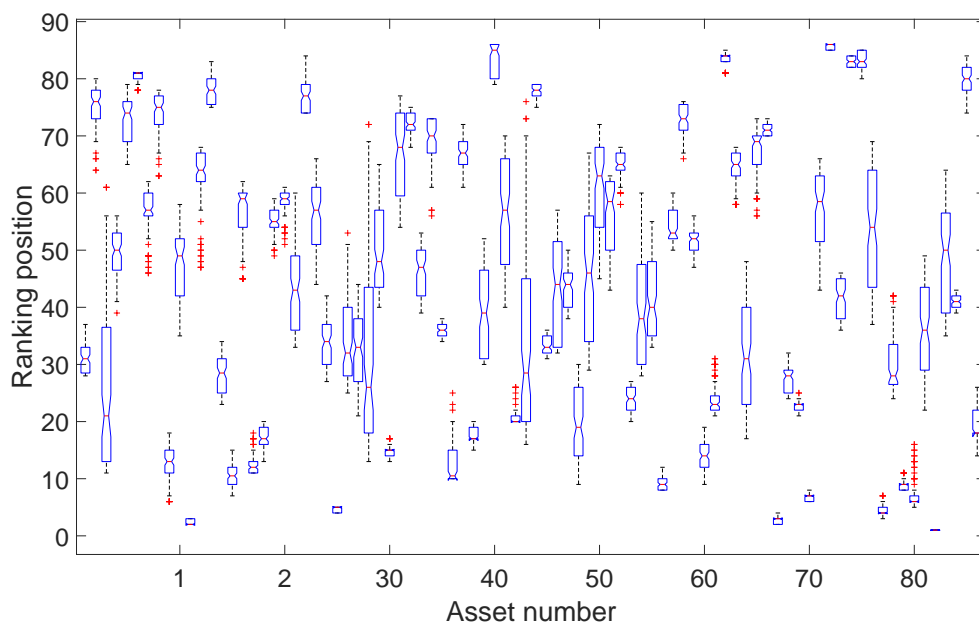


Figure 6: Figure reports the distribution of nodes' rankings based on \mathcal{R}_i with respect to ζ . For each distribution, the set of outcomes is given by the rankings of \mathcal{R}_i computed for alternative values of ζ . Results regard the asset-tree at the end of 2007.

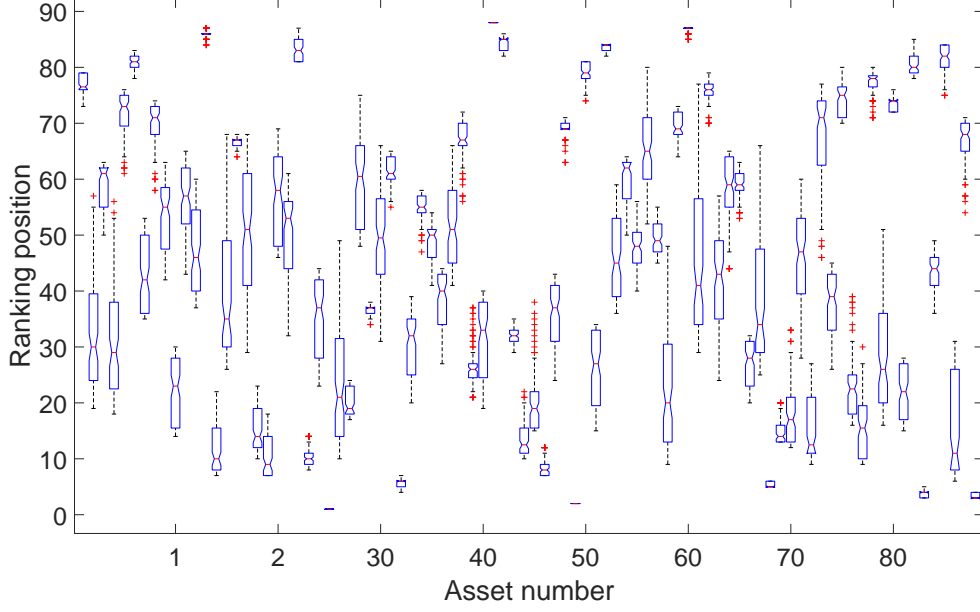


Figure 7: Figure reports the distribution of nodes' rankings based on \mathcal{R}_i with respect to ζ . For each distribution, the set of outcomes is given by the rankings of \mathcal{R}_i computed for alternative values of ζ . Results regard the asset-tree at the end of 2008.

6.2. US corporate network. We now move to the analysis of the network of US top corporates according to Forbes in 1999. We start by assessing the relevance of each corporate by using the risk-dependent centrality \mathcal{R}_i for two different values of the infectability ζ . Reminding that ζ ranges in $(0, 1]$, we assume that $\zeta = 0.01$ represents a low infectability rate and $\zeta = 1$ represents a high infectability rate. In Table 2, we collect the top 20 Corporates according to their ranking in risk-dependent centrality for the weighted network. As we can see, Chase Manhattan Corp. is the top most central corporate at both low and high values of infectability. Sara Lee Corp. and Bell Atlantic Corp. switch their rankings from low to high infectability although they still remain at the top. Indeed Chase Manhattan Corp. has the highest strength ($s_i = 41$) in the whole network. Moreover, it belongs to a very high number of triangles ($t_i = 67$), whose weight ($t_i^w = 150$) is the highest value in the network. (The highest number of triangles is $t_i = 70$ for American Express, which is the fourth in the ranking at low external risk.) Notice that the weight of a triangle is computed as $t_i^w = \frac{1}{2}[W^3]_{ii}$. We should notice that for a triangle we compute the weighted number of cycles of length 3, which is the product of the edges weights. The total weight is the sum over all the triangles to which the node takes part. This definition is consistent with those provided by Onnela ([84]).

Moreover, we can qualitatively explain why Bell Atlantic Corp. and Sara Lee Corp. switch their rankings: in fact, Bell Atlantic Corp. has a higher strength than Sara Lee Corp. ($s_i = 39$ and 37, respectively) but Sara Lee Corp. belongs to a higher number of triangles than Bell Atlantic Corp. ($t_i = 69$ and 53, respectively), even if their weights are, respectively, 106 and

116. Indeed, we expect that at low external risk the risk-dependent centrality is determined by the node strength while, at high external risk, the risk-dependent centrality is determined by its participation in higher order walks (mainly depending on the number of triangles).

Being at the top of the ranking, in principle, these three corporates should be the most exposed to the risk, both in terms of circulability and transmissibility, among the top US corporations. However, it could be argued that, if a corporation does not change its ranking from low to high infectability, the external stress on the network does not affect significantly its behavior and, even if very exposed to a high level of risk, it is stable enough as to manage such risk in its benefit.

For instance, although during the “credit crunch” crisis in 2008 pure investment banks such as Bear Stearns and Lehman Brothers suffered important losses, JP Morgan Chase&Co. – which emerged from the merging of Chase Manhattan Corporation with JP Morgan & Co. in 2000 – weathered the crisis well. This was mainly due to the fact that this bank combined investment and commercial banking. JP Morgan Chase&Co. is currently the largest bank in the world in terms of market capitalization.

Similarly, in early 1997, the CEO of Bell Atlantic, one of the most important American corporate of telecommunications, orchestrated its merger with NYNEX and the new company’s assets serviced 25% of the overall U.S. market. Since then it continued its diversified international investment strategy, acquiring, for instance, in early 2000’s GTE, which operated telecommunications companies across most of the rest of the country that was not already in Bell Atlantic’s footprint.

Sara Lee Corp. is an American consumer-goods corporation. It sells its frozen and packaged foods in more than 180 countries. Including all its spin-offs, Sara Lee raised more than 3.7 billion in proceeds as part of the company’s transformation plan begun in early 2000’s.

In contrast, it calls immediately the attention the case of Lucent Technologies Inc. This corporate, operating in the telecommunication market, rose 13 positions in the ranking of the risk-dependent centrality \mathcal{R}_i from ζ low, becoming the fourth company in the top ranking when ζ is high.

Lucent Technology represents a unique case of study, as pointed out by Lazonik and March in [71]. Indeed, the central question the authors pose is: *Can an ‘old economy’ company comprised predominantly of employees and executive managers whose careers developed within a regulated business framework make the necessary changes for success when facing global competitors in a deregulated environment? Incremental change would not be sufficient, more significant change was necessary to benefit from opportunities in the growing global telecommunications equipment market.* This fact is essential in our case where we are studying a network in which links are weighted by common directors whose ability or inability in facing new market challenges become crucial for the growth of a company. Indeed, in 1999 Lucent Technologies Inc. had revenues of \$38.3 billion, net income of \$4.8 billion, and 153,000 employees and was at the top of telecommunications equipment companies. It was larger and more profitable than its major competitors, such as Nortel, Alcatel, and Ericsson. However, in 2006 Lucent’s revenues dropped dramatically to only \$8.8 billion and the number of employees at the company shrunk to 29,800. This led to the company’s merger on December 2006 to form Alcatel-Lucent, which made Lucent a wholly owned subsidiary of Alcatel.

Another interesting example is provided by Alcoa Inc. This firm occupies the 55th position

in the ranking for low ζ but it climbs the ranking up to the 8th position for high ζ . Immediately after the year our analysis refers to, Alcoa purchased an 8% stake of Aluminum Corporation of China (Chalco), with the aim to settle a strategic alliance with the China's largest aluminum producer (see page 66 of [61]). This strategic investment exposed the company to a considerably high level of risk. However, Alcoa sold all its stake in Chalco in 2007.

Table 2: Top 20 US Companies in terms of \mathcal{R}_i for low ($\zeta = 0.01$) and high ($\zeta = 1.00$) risk in the weighted version of the US corporate network. In bold we report the companies that appear either at low risk or at high risk.

| Ranking | Low external risk ($\zeta = 0.01$) | High external risk ($\zeta = 1.00$) |
|---------|--------------------------------------|---------------------------------------|
| 1 | CHASE MANHATTAN CORP | CHASE MANHATTAN CORP |
| 2 | BELL ATLANTIC CORP | SARA LEE CORP |
| 3 | SARA LEE CORP | BELL ATLANTIC CORP |
| 4 | AMERICAN EXPRESS CO | LUCENT TECHNOLOGIES INC |
| 5 | BANK OF AMERICA CORP | CUMMINS ENGINE CO INC |
| 6 | CUMMINS ENGINE CO INC | AMERITECH CORP |
| 7 | EQUIFAX INC | AMERICAN EXPRESS CO |
| 8 | SUNTRUST BANKS INC | ALCOA INC |
| 9 | AMERITECH CORP | PROCTER & GAMBLE CO |
| 10 | PROCTER & GAMBLE CO | JP MORGAN & CO INC |
| 11 | XEROX CORP | XEROX CORP |
| 12 | WELLS FARGO & CO NEW | SEARS ROEBUCK & CO |
| 13 | CITIGROUP INC | CITIGROUP INC |
| 14 | AON CORP | RYDER SYSTEM INC |
| 15 | BANK ONE CORP | GTE CORP |
| 16 | JP MORGAN & CO INC | ALLIED SIGNAL INC |
| 17 | LUCENT TECHNOLOGIES INC | UNION CARBIDE CORP_ NEW |
| 18 | SEARS ROEBUCK & CO | EQUIFAX INC |
| 19 | ALLIED SIGNAL INC | WARNER LAMBERT CO |
| 20 | AMR CORP | JOHNSON & JOHNSON |

We devote the rest of this section to the investigation about whether such a significant increase of the risk-dependent centrality is a proxy of the vulnerability of the corporate to financial infections propagating on the corporate network.

At first, we should remark the fact that the network we are considering here was built based on data corresponding to year 1999. At this year the level of stress of the international economic system was relatively high due to the fact that the East Asian financial crisis occurred in the years 1997–1998, which was also followed by the Russian default of 1998. The two aforementioned financial crises had a ripple effect also on the US market. In the literature, for instance, is well-documented the so-called “fire-sale” FDI (Foreign Direct Investment) phenomenon, that is, the surge of massive foreign acquisitions of domestic firms during a financial crisis ([35, 4]). Thus, the level of stress and infectability of the system in 1999 is

expected to be significantly larger than in the subsequent years when the effects of these crises gradually relaxed. Therefore, we proceed our analysis by considering that the level of infectability in 1999 is high and we investigate the effects of relaxing such a condition to lower levels of stress. That is, we start by assuming that in 1999 the external market turmoil could be represented by a value of $\zeta = 1$ and we want to find out how the companies change their ranking position in term of \mathcal{C}_i and \mathcal{T}_i as ζ vanishes.

In order to accomplish this task, we need to embed our analysis in a temporal framework. To this purpose, we consider a period of five years from 1998 to 2002 and we partition this period into a given number of subintervals, e.g., for the sake of simplicity, five years. Then we assign to each one a different value of the parameter γ , according to the environmental conditions of the market. In this way, we describe the evolution of the market by using the contagion model with different initial setups of the infectability rates (one for each subinterval). We do not mean to set up a single initial condition describing a unique spreading phenomenon over time with the same value of γ , according to (3.3).

Now, let us consider [Figure 8](#).

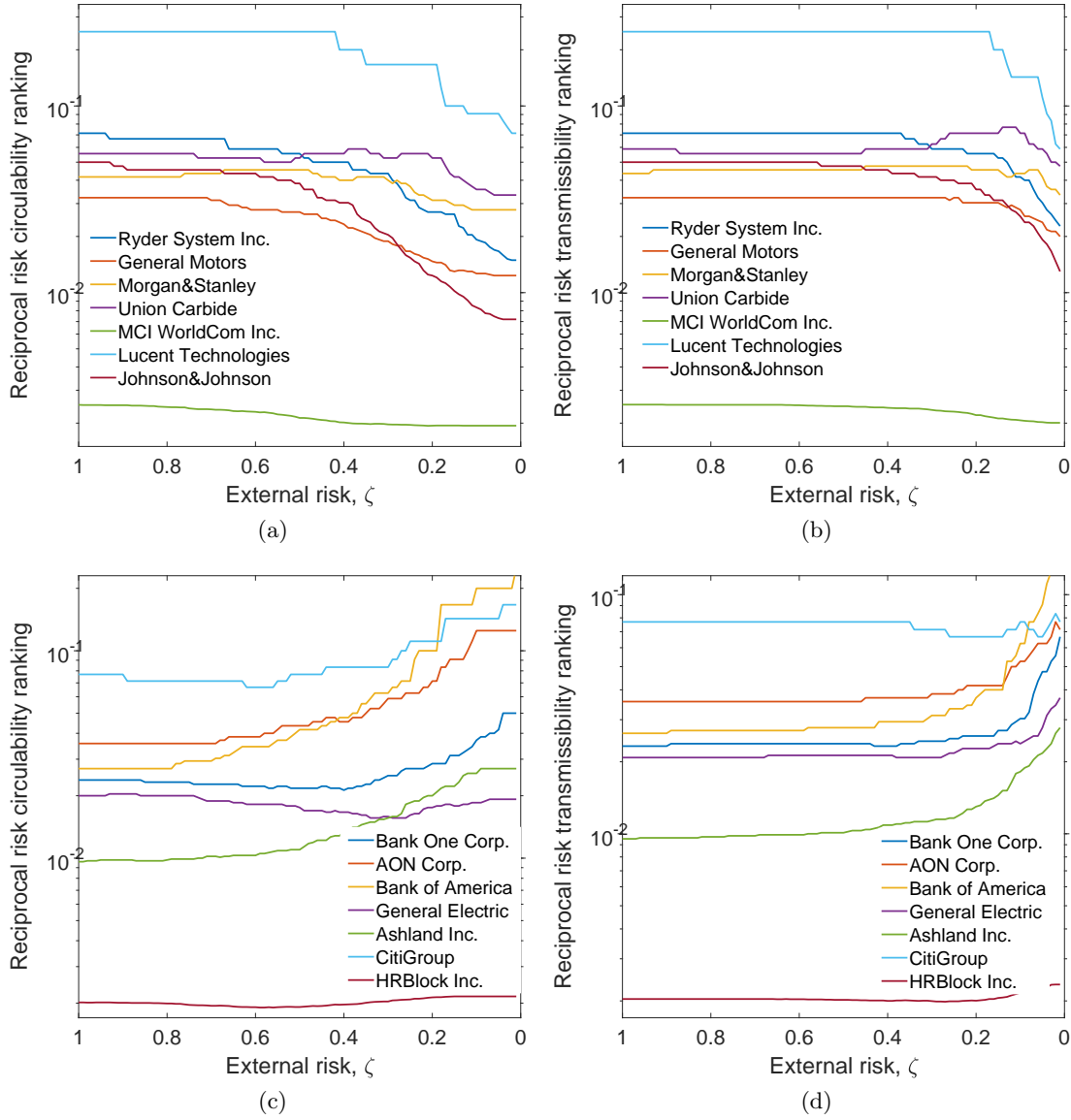


Figure 8: Illustration of a group of companies for which both circulability and transmissibility risk-dependent centralities decrease (a and b) or increase (c and d) with the decay of the external risk γ in the weighted version of the US corporate network. Notice the reverse x-label scale.

We illustrate the change in the ranking position, both in circulability ((a) and (c)) and transmissibility ((b) and (d)), for two groups of seven companies. Specifically, on the vertical axis we have the reciprocal of the ranking position and on the horizontal axis we have the values of ζ , in a reverse scale, from 1 to 0. As the global infectability of the system drops from 1 to 0, we have noticed that for all these companies there is a significantly high rank

correlation between \mathcal{R}_i and \mathcal{T}_i . The Spearman correlation coefficient is larger than 0.99. Thus, we focus our analysis on the two components of the risk-dependent centrality, namely \mathcal{C}_i and \mathcal{T}_i . High values on the vertical axis correspond to high risk-centrality values.

In particular, Figures 8 (a) and (b) display the ranking for a sample of seven companies which decrease their risk level from $\zeta = 1$ to $\zeta = 0$. In a similar way, Figures 8 (c) and (d), show the same rankings for seven companies which increase significantly their risk level.

Let us briefly explain the meaning of plots in Figure 8.

The corporates in plots (a) and (b) are those having a relatively high risk in 1999 when the infectability of the system was very large, and whose risk drops when the effects of the crises affecting the system were relaxed. In contrast, those companies in plots (c) and (d) have a relatively low level of risk at the time of the crises but subsequently increase such level when the infectability of system drops.

It is not an easy task to find quantitative parameters tied to the increase of risk in these corporations when the infectability of the global financial system is high. Nonetheless, according to the *OECD Principles of Corporate Governance*, corporations should be run, first and foremost, in the interests of shareholders (OECD 1999). Therefore, companies should work to increase their shareholder values. Increasing shareholders value cannot be done without risk. It is known that in the shareholder value model, companies usually take more risk than needed in order to maximize shareholders value creation (SVC). As a consequence of this additional risk, companies acquire debts which could make them unstable and more exposed to the risk of bankruptcy. Acquiring large debts is seen as conducive to increasing shareholder value due to the potential of the company to increase value when it has started from a low baseline. Thus, there is a relation between SVC and risk, because in searching for large SVC the companies increase their risks to attract more investors and increasing potential value gain. However, the risk also puts the company in a more vulnerable position to bankruptcy and collapse.

SVCs of the companies in the S&P 500 have been collected by Fernandez and Reinoso for the period 1998-2002, which is of great value for the current work as the corporate network analyzed here is based on data of 1999. In Table 3 we give the ranking of the companies studied in this section by their SVC for every year in the period 1998-2002. For Union Carbide and MCI World we used the data reported for Dow Chemicals and Verizons, respectively, as the original companies were acquired or merged to form the new ones. Here we focus on the trend of these companies in terms of the SVC for the period 1998-2002. Then, in order to quantify the trend of SVC over time and to keep a relation with the level of infectability in the system, we consider the Pearson correlation coefficient r between SVC-based ranking and the reciprocal of the year. In this case, a negative value of r indicates that the corresponding company decreases the risk from 1998 to 2002. That is, the company decreases its risk when the infectability decreases in the system. On the other hand, a positive value of r indicates that the corresponding company increases its risk when the global external infectability decreases.

As can be seen in Table 3, only one out of seven companies, for which \mathcal{C}_i and \mathcal{T}_i decrease when ζ drops, does not display negative Pearson correlation coefficient. Similarly, two out of seven companies, that increase their risk, do not display positive values of r .

In other words, the risk described by the model and the SVC-based risk move in the same direction over time. For instance, those companies predicted by \mathcal{C}_i and \mathcal{T}_i to increase their

risk are those for which the SVC-based risk increased from 1998 to 2002 when the level of stress is also dropped.

Table 3: Position of the companies in the ranking based on the shareholder value creation (SVC) in the period 1998-2002. r indicates the Pearson correlation coefficient of SVC-based ranking vs. the reciprocal of the year indicating a positive or negative trend in the SVC for this period. For Union Carbide (*) and MCI World (**) we used the data reported for Dow Chemicals and Verizons, respectively, see text for explanation. Risk refers to the increase (I) or decrease (D) of circulability and transmissibility of that corporate in the network with the increase of the external risk.

| Corporate | | | | | | | Risk |
|---------------------|------|------|------|------|------|---------------|------|
| | 1998 | 1999 | 2000 | 2001 | 2002 | r | |
| Ryder System | 334 | 235 | 294 | 137 | 92 | 0.899 | D |
| General Motors | 60 | 48 | 453 | 345 | 411 | -0.810 | D |
| Morgan Stanley | 80 | 17 | 280 | 476 | 471 | -0.918 | D |
| Union Carbide* | 435 | 47 | 422 | 359 | 370 | -0.180 | D |
| MCI World** | 45 | 49 | 463 | 446 | 482 | -0.879 | D |
| Lucent Technologies | 3 | 18 | 483 | 473 | 464 | -0.858 | D |
| Johnson & Johnson | 24 | 70 | 54 | 7 | 480 | -0.675 | D |
| Bank One | 348 | 466 | 93 | 126 | 383 | 0.259 | I |
| AON Corporation | 374 | 196 | 365 | 195 | 372 | 0.008 | I |
| Bank of America | 432 | 464 | 441 | 3 | 2 | 0.859 | I |
| General Electric | 5 | 3 | 474 | 492 | 500 | -0.880 | I |
| Ashland Inc. | 333 | 320 | 236 | 115 | 238 | 0.717 | I |
| CitiGroup | 459 | 8 | 7 | 460 | 494 | -0.325 | I |
| H&R Block Inc. | 305 | 257 | 295 | 19 | 243 | 0.488 | I |

Let us conclude with the following observation. Even if “good” companies increase their risk-centrality ranking as ζ vanishes, it is worth noting that this occurs when the global stress in the market is very low. When the infectability rate is very low, the absolute probability of getting infected also remains very low for both “good” and “bad” companies. To show this fact, let us consider that, according to our model, the probability that a given corporate is not affected by a crisis propagating inside the network is given by

$$1 - x_i(t) = \alpha e^{-\frac{p}{\alpha}(\mathcal{R}_i - 1)}$$

where again p and $\alpha = 1 - p$ are the initial probabilities to have infected and not-infected nodes, respectively. Hence, the ratio between the probabilities of two nodes i and j to pass successfully through a crisis is given by

$$\frac{1 - x_i(t)}{1 - x_j(t)} = e^{\frac{p}{\alpha}(\mathcal{R}_j - \mathcal{R}_i)}$$

If we compute these ratios for different couples of corporates operating in a similar sector, a “good” one and a “bad” one, we get [Figure 9](#).

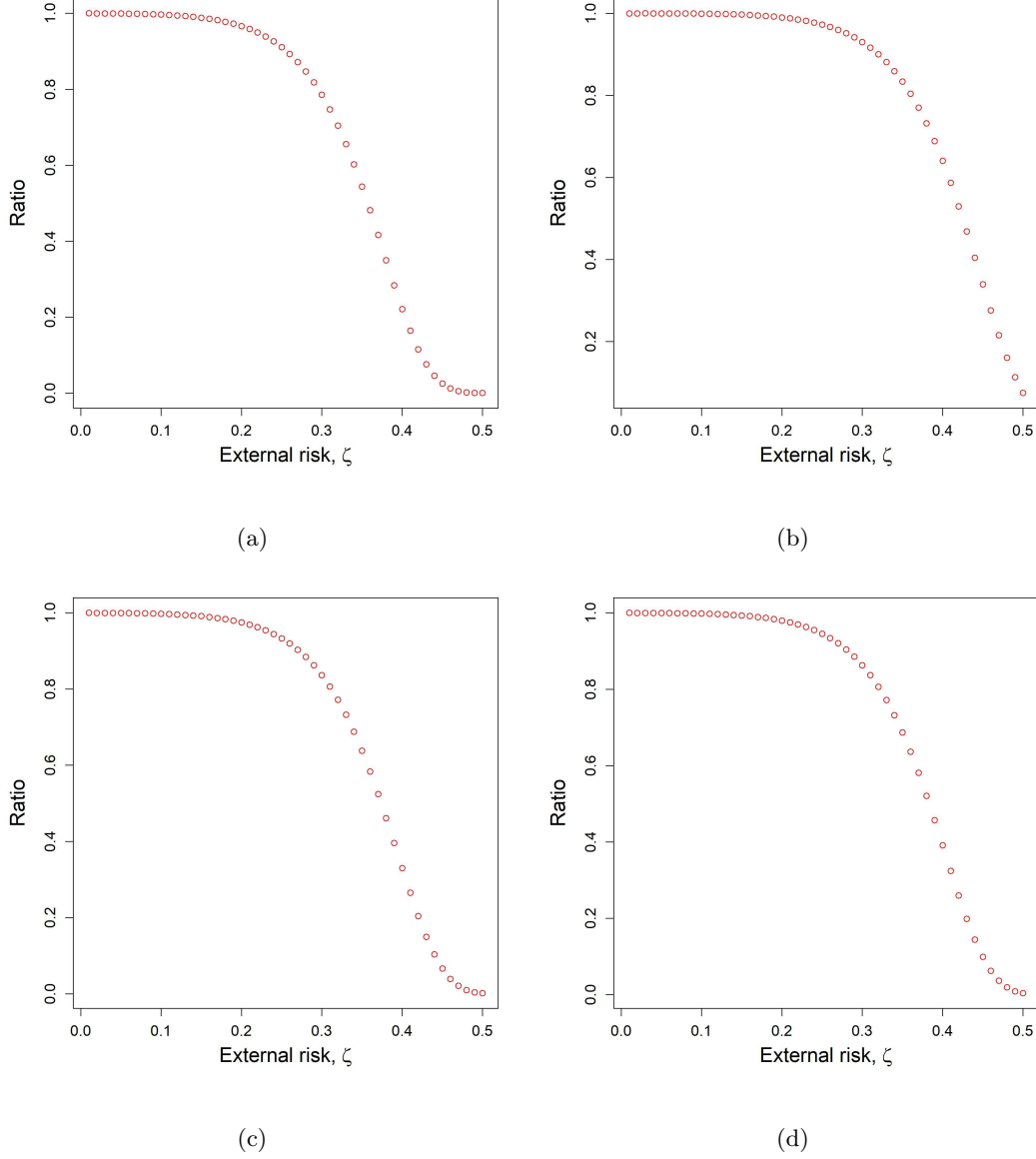


Figure 9: Figures display the ratios between the probabilities of not being infected by a crisis for different couples of Corporates: a) Lucent Technologies Inc. over General Electric Co. b) Morgan Stanley Co. over Bank One Corp. c) Union Carbide Corp. New over Ashland Inc. d) American Express Co. over Bank of America Corp.

These plots show that, as expected, at low ζ the probabilities of not being infected by a

crisis is the same for both high and low risk-centrality companies. But this ratio decreases very quickly as ζ increases and this means that for Lucent Technologies, Morgan Stanley, Union Carbide and American Express the probabilities to stay safe during a crisis are very small if compared with the analogous probabilities for General Electric, Bank One, Ashland and Bank of America, respectively.

7. Ranking interlacement. During the analysis of the two real-world networks studied above, we have noticed that with the change of ζ some corporates vary their ranking significantly, to the point of changing their positions relative to each other. For instance, in [Figure 10](#) we illustrate six pairs of corporates that interlace their positions with the change of the global infectability in the network. In the first pair, [Figure 10\(a\)](#), we see that at low levels of infectability, i.e., $\zeta \rightarrow 0$, J.P. Morgan&Co Inc. (red) occupies a position in the ranking of \mathcal{C}_i more at the bottom than Bank of America Corp. (blue). That is, at low global infectability J.P. Morgan&Co is exposed to less risk than Bank of America. However, when the global infectability in the network increases ($\zeta \rightarrow 1$), Bank of America is exposed to less risk than J.P. Morgan&Co. A similar interlacement is observed between the other couples in [Figure 10](#). For instance, in [Figure 10\(f\)](#), the interlacement between rankings for General Motors Corp. (red) and Boeing Co. (blue) occurs at a smaller value of ζ than for the previous cases. Before proceeding with the analysis of this phenomenon we would like to remark that the existence of ranking interlacement means that the ranking of the nodes in a network based on the risk-dependent centralities is not unique and fixed as in the case of other classical centrality measures, e.g., degree, eigenvector, closeness, betweenness. Here instead the ranking of nodes depends on the global external conditions to which the network is submitted.

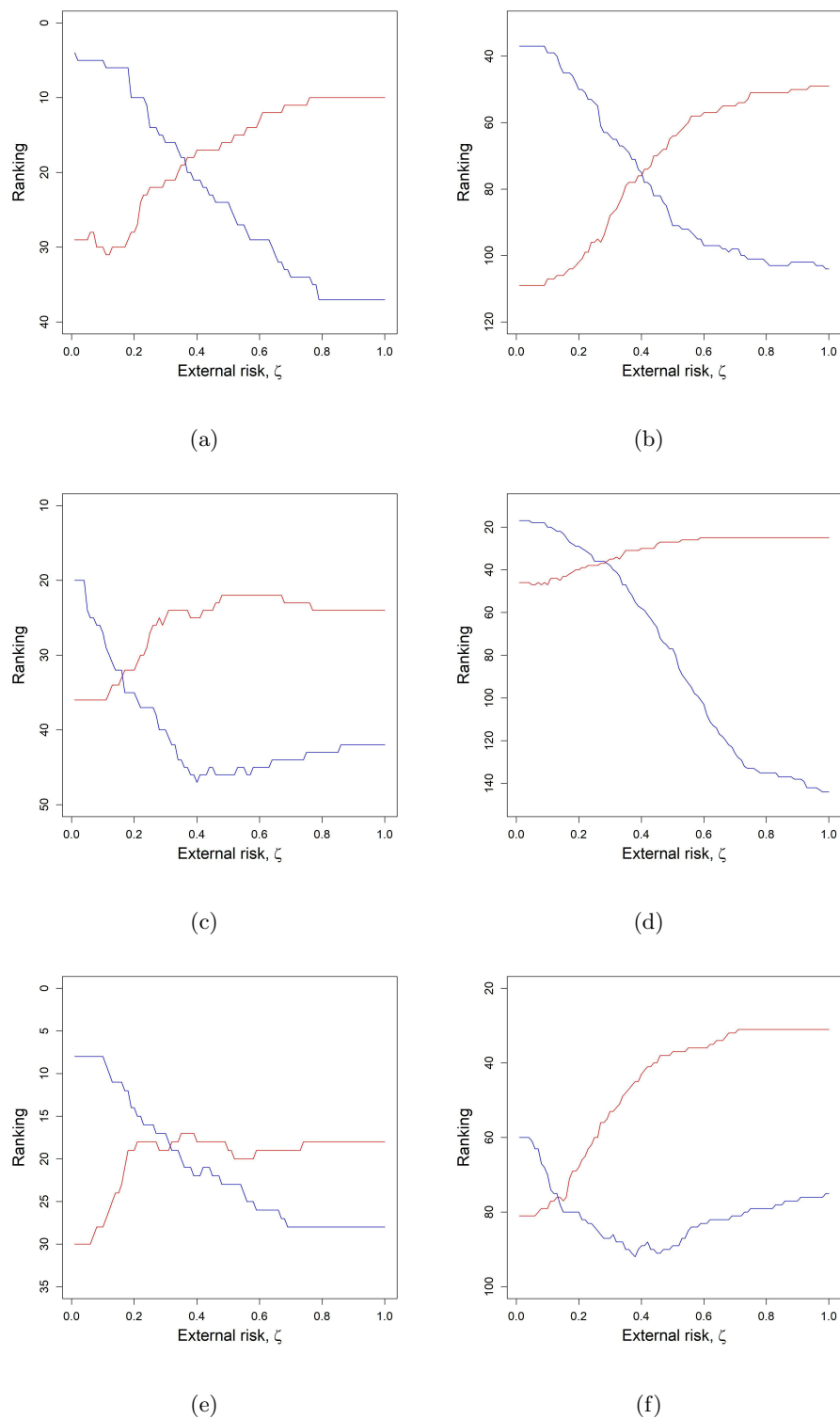


Figure 10: Illustration of the Circulability Ranking Interlacement for a) J.P. Morgan&Co Inc. (red) and Bank of America Corp. (blue) b) Pfizer Inc. (red) and Ashland Inc (blue) c) Morgan Stanley & Co. (red) and Bank One Corp. (blue) d) AT&T Corp. (red) and Airtouch Communications Inc. (blue) e) Union Carbide Corp. New (red) and AON Corp. (blue) f) General Motors Corp. (red) and Boeing Co. (blue)

In order to shed light on the issue of ranking interlacement we will make use of different representations of the risk-dependent total communicability $\mathcal{R}_i(\zeta)$ and circulability $\mathcal{C}_i(\zeta)$ measures (the transmissibility is obtained as the difference of these two and can be treated accordingly). First, expanding the matrix exponential in a power series gives the representation

$$(7.1) \quad \mathcal{R}_i(\zeta) = \left(e^{\zeta A} \mathbf{1} \right)_i = \sum_{k=0}^{\infty} \frac{\zeta^k}{k!} w_i^{(k)},$$

where $w_i^{(k)} = \left(A^k \mathbf{1} \right)_i$ denotes the number of walks of length k starting from the node i , with $w_i^{(0)} = 1$. In particular, $w_i^{(1)} = k_i$, the degree of node i . Similarly,

$$(7.2) \quad \mathcal{C}_i(\zeta) = \left(e^{\zeta A} \right)_{ii} = \sum_{k=0}^{\infty} \frac{\zeta^k}{k!} w_{i,i}^{(k)},$$

where now $w_{i,i}^{(k)} = \left(A^k \right)_{ii}$ is the number of closed walks of length k through node i ; in particular, $w_{i,i}^{(0)} = 1$, $w_{i,i}^{(1)} = 0$, $w_{i,i}^{(2)} = k_i$, and $w_{i,i}^{(3)} = 2t_i$, where t_i is the number of triangles node i participates in.

Second, we recall that the spectral theorem yields the formulas

$$(7.3) \quad \mathcal{R}_i(\zeta) = \sum_{k=1}^n e^{\zeta \lambda_k} \left(\psi_k^T \mathbf{1} \right) \psi_{k,i}, \quad \mathcal{C}_i(\zeta) = \sum_{k=1}^n e^{\zeta \lambda_k} (\psi_{k,i})^2.$$

Using (7.1)-(7.2), we readily see that both functions of ζ are *absolutely monotonic* for $\zeta > 0$, i.e. they are positive and infinitely differentiable on $(0, \infty)$, with all the derivatives being nonnegative. In particular, both functions are strictly increasing and strictly convex (for the circulability, this last property holds provided Γ is not a tree).

Definition 7.1. We say that the rankings of node i and node j based on the circulability interlace at $\zeta^* > 0$ if $\mathcal{C}_i(\zeta^*) = \mathcal{C}_j(\zeta^*)$ and there exists an $\varepsilon > 0$ such that $\mathcal{C}_i(\zeta) - \mathcal{C}_j(\zeta)$ changes sign exactly once in $(\zeta^* - \varepsilon, \zeta^* + \varepsilon)$.

In other words, nodes i and j interlace at ζ^* if and only if $\mathcal{C}_i(\zeta^*) = \mathcal{C}_j(\zeta^*)$ and the two functions are not identical (on an open neighborhood of ζ^* or, equivalently, for all ζ).

An analogous definition can be given for the ranking based on other ζ -dependent measures, like the total communicability $\mathcal{R}_i(\zeta)$. In the following we limit our discussion to the interlacing of rankings according to the circulability, but analogous observations hold for the total communicability and transmissibility functions.

Identifying the interlacing points (if they exist) amounts to finding the roots of the transcendental equation $\mathcal{C}_i(\zeta) - \mathcal{C}_j(\zeta) = 0$, or

$$\Psi(\zeta) := \sum_{k=1}^n e^{\zeta \lambda_k} [\psi_{k,i}^2 - \psi_{k,j}^2] = 0.$$

Even if we knew the eigenvalues and eigenvectors of A explicitly, there is no general closed form expression for the roots of the transcendental function Ψ . Of course one could

resort to numerical root-finding techniques, but this would be impractical for large networks. Here and below we give a qualitative discussion followed by a heuristic approach that yields approximations that seem to work well in practice.

We begin with the following result. It applies to both circulability and total communicability-based rankings, and in fact for a much larger class of parameter-dependent centrality ranking functions, including Katz centrality [63]. We remind the reader that we restrict the risk rate ζ to positive values.

Theorem 7.2. *The number of rank interlacing points is always finite (possibly zero).*

Proof. Let us assume that there is at least one pair of nodes, i and j , whose rankings interlace, otherwise $\Psi(\zeta) = 0$ has no positive roots. Observe that the ranking of node i provided by $\mathcal{C}_i(\zeta)$ is identical to that obtained using

$$\hat{\mathcal{C}}_i(\zeta) = e^{-\zeta\lambda_1}\mathcal{C}_i(\zeta) = \psi_{1,i}^2 + \sum_{k=2}^n e^{\zeta(\lambda_k - \lambda_1)}\psi_{k,i}^2.$$

As this quantity tends monotonically to $\psi_{1,i}^2$ for $\zeta \rightarrow \infty$, there exists a $\bar{\zeta}$ such that no rank interlacing can occur for $\zeta > \bar{\zeta}$, since all the node rankings must stabilize on the eigenvector rankings in the large ζ limit, and there are finitely many nodes. Hence, all interlacing points must fall within the compact interval $[0, \bar{\zeta}]$. Suppose that the number of interlacing points is infinite. By the Bolzano-Weierstrass Theorem, this set has a point of accumulation. But since $\hat{\Psi}(\zeta) := e^{-\zeta\lambda_1}\Psi(\zeta)$ is analytic, and zero on this set, it must be identically zero everywhere, which contradicts the assumption that there is at least one interlacing point in $(0, \infty)$. ■

An obvious sufficient condition for the existence of at least one interlacing point for the pair of nodes i and j is that $k_i \geq k_j$ (or $k_j \geq k_i$) while $\psi_{1,i} < \psi_{1,j}$ (resp., $\psi_{1,i} > \psi_{1,j}$). In this case, the number of interlacing points is necessarily odd. That the above condition is not necessary is made clear considering the possibility of an even number of interlacing points. A necessary condition for the existence of at least one interlacing point is that there exist at least two values of k , say k_1 and k_2 , for which $(A^{k_1})_{ii} - (A^{k_1})_{jj}$ and $(A^{k_2})_{ii} - (A^{k_2})_{jj}$ have different sign. Indeed, it is obvious from (7.1)–(7.2) that if (say) $(A^k)_{ii} \geq (A^k)_{jj}$ for all k , then no rank interlacing point exists. That this condition may not be sufficient is suggested by the fact that the series expansions contain an infinity of terms.

We mention that the same problem has been studied, for a different centrality function (the Katz resolvent), by E. Horton, K. Kloster, and B. D. Sullivan, independently of us [66].

7.1. A back of envelop approach. We now consider heuristics based on truncated series expansions. Let $k_0 \geq 3$ be the smallest value of k such that the sequence of values $\{(A^k)_{ii} - (A^k)_{jj}\}_{k \geq 2}$ undergoes a sign change (here zero is considered positive). If no such k_0 exists, then no interlacing can take place, as we already observed. We consider approximating $\mathcal{C}_i(\zeta)$ with its truncation to an order $k \geq k_0$:

$$(7.4) \quad \mathcal{C}_i(\zeta) \approx 1 + \frac{1}{2!}\zeta^2 w_{i,i}^{(2)} + \frac{1}{3!}\zeta^3 w_{i,i}^{(3)} + \cdots + \frac{1}{k!}\zeta^k w_{i,i}^{(k)} = \tilde{\mathcal{C}}_i(\zeta),$$

where we recall that $w_{i,i}^{(k)} = (A^k)_{ii}$. We emphasize that this polynomial approximation assumes that ζ is small, since the error in it is $O(\zeta^{k+1})$. In alternative we can also use as a surrogate

for \mathcal{C}_i the same polynomial shifted by 1 and divided by ζ^2 :

$$\frac{\tilde{\mathcal{C}}_i(\zeta) - 1}{\zeta^2} = \frac{1}{2!}w_{i,i}^{(2)} + \frac{1}{3!}\zeta w_{i,i}^{(3)} + \cdots + \frac{1}{k!}\zeta^{k-2}w_{i,i}^{(k)},$$

where now the error is $O(\zeta^{k-1})$. We can now use these polynomial approximations to try to locate, approximately, any interlacing points sufficiently small in magnitude. This requires finding the (positive) roots, if any, of the polynomial equation of degree $k - 2$:

$$(7.5) \quad q(\zeta) = \frac{(w_{i,i}^{(k)} - w_{j,j}^{(k)})}{k!}\zeta^{k-2} + \frac{(w_{i,i}^{(k-1)} - w_{j,j}^{(k-1)})}{(k-1)!}\zeta^{k-3} + \cdots + \frac{(w_{i,i}^{(3)} - w_{j,j}^{(3)})}{3!}\zeta + \frac{(w_{i,i}^{(2)} - w_{j,j}^{(2)})}{2!} = 0.$$

It is well known that for degree greater than or equal to 5 there is no closed form expression of the solutions of an algebraic equation involving only arithmetic operations and root extractions, so in general if $k \geq 7$ we will have to resort to numerical methods for solving (7.5). Evaluation of the coefficients requires computing the diagonal entries of powers of the adjacency matrix A , which can be expensive for very large graphs and large values of k .

As the simplest possible example, we consider the case where $w_{i,i}^{(2)} > w_{j,j}^{(2)}$ and $w_{i,i}^{(3)} < w_{j,j}^{(3)}$ (or vice-versa), i.e., $k_0 = 3$. Taking $k = k_0$, equation (7.5) becomes the linear equation

$$\frac{(w_{i,i}^{(3)} - w_{j,j}^{(3)})}{3!}\zeta + \frac{(w_{i,i}^{(2)} - w_{j,j}^{(2)})}{2!} = 0,$$

which admits the unique solution $\zeta^* = \frac{3(w_{i,i}^{(2)} - w_{j,j}^{(2)})}{w_{i,i}^{(3)} - w_{j,j}^{(3)}}$, which is of course positive. In terms of the degree of the nodes and the number of triangles in which they take place, this can be written in the form:

$$(7.6) \quad \zeta^* = \frac{3}{2} \left| \frac{k_i - k_j}{t_i - t_j} \right|.$$

In the case of weighted networks, the degree is replaced by the weighted degree or strength, and the number of triangles is replaced by the weighted number of cycles of length 3, i.e., the weight of a cycle of length 3 is the product of the weights at its three edges. A priori, there is no reason to expect that this value is close to an actual interlacing point (assuming it even exists), since the behavior of higher order terms may more than offset the influence of the negative term involving $t_i - t_j$. Better approximations might be obtained by considering higher order approximations; for example using $k = 4$ leads to an easily solved quadratic equation in ζ , $k = 5$ leads to a cubic, and so forth. In any case, these are heuristics whose usefulness can only be assessed experimentally on concrete examples. We emphasize that the use of power series truncation requires knowledge of k_0 , since truncating the series at orders lower than k_0 would lead to an equation devoid of positive solutions and therefore to concluding that no interlacing points exist for a given pair of nodes, even if such points do exist.

It is also worth recalling Descartes's Rule of Signs, according to which the number of positive real roots of a polynomial (counted with their multiplicities) is equal to the number

of sign changes in the (nonzero) coefficients or less than that by an even whole number, when the powers are ordered in descending order. If, moreover, the polynomial is known to have only real roots (as in the case of a symmetric adjacency matrix, i.e., of undirected networks) then the number of sign changes is exactly equal to the number of positive roots. It is then obvious that if the power series is truncated at order k_0 , i.e., as soon as we observe the first sign change in the coefficients, then there will be exactly one positive root and therefore only one (approximate) interlacing point can be found by this method. A polynomial truncation of higher degree $k > k_0$ may have more than one positive root, depending on the number of changes in the coefficients (assuming the network is undirected). We will come back to this case shortly.

To exemplify the previous finding let us consider a pair of nodes with a small difference in their degree, e.g., $k_i - k_j = 2$, then $-(k_i - 2)^2 \leq (t_i - t_j) \leq k_i^2$, such that if, for instance, $k_i \leq 10$ and we let ζ vary from 0 to 0.1 we obtain the plot given in Figure 11(a). As can be seen there are certain values of $\Delta = t_i - t_j < 0$ for which we can obtain positive and negative values of $\mathcal{C}_i - \mathcal{C}_j$. This is illustrated in Figure 11(b) where we can see that when $-100 \leq \Delta \leq -40$ there are both positive and negative values of $\mathcal{C}_i - \mathcal{C}_j$. In other words, it is possible to find pairs of nodes for which $\mathcal{C}_i(\zeta_1) > \mathcal{C}_j(\zeta_1)$ and then $\mathcal{C}_i(\zeta_2) < \mathcal{C}_j(\zeta_2)$, which means that these nodes will change their ranking position in terms of the risk-dependent centrality when the values of ζ change even for a relatively narrow window. Notice that if $k_i - k_j = 2$, and $\Delta \geq -30$ such change is not observed for the corresponding range of ζ analyzed.

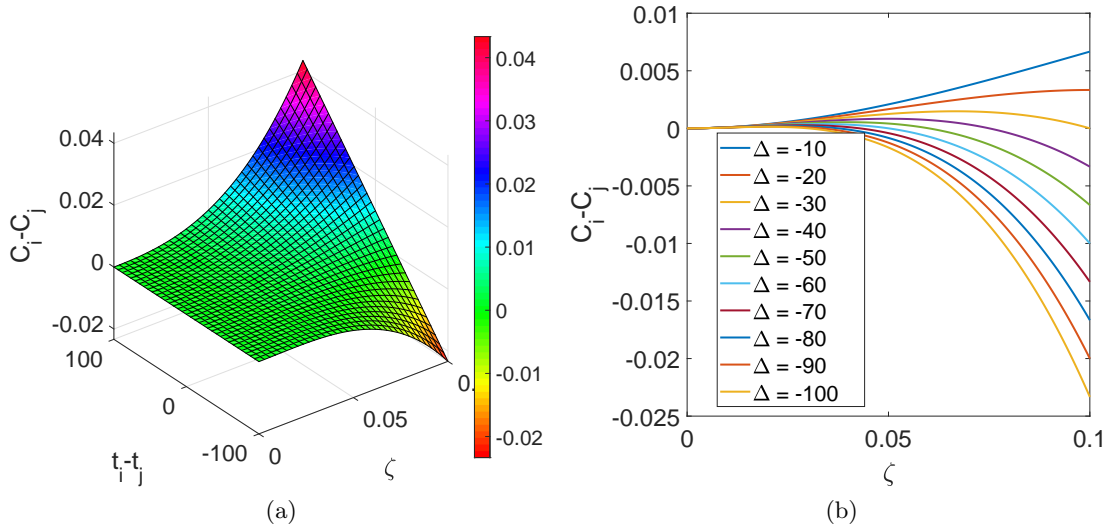


Figure 11: (a) Illustration of the change in the difference in the risk-dependent centrality of nodes having a small difference in degrees, $k_i - k_j = 2$, as a function of the difference in the number of triangles, $t_i - t_j$ and of the network infectivity (risk) ζ . (b) Some of the curves obtained for $k_i - k_j = 2$ and a given value of $\Delta = t_i - t_j$ as a function of ζ .

If we now consider a large difference in the node degrees, e.g., $k_i - k_j = 100$, and the same

range of change for the difference in the number of triangles, e.g., $-100 \leq \Delta \leq 100$ we do not observe any variation in the ranking of pairs of nodes as can be seen in Figure 12(a). In this case the range of Δ must be increased dramatically to obtain inversions in the ranking of pairs of nodes (see Figure 12(b)).

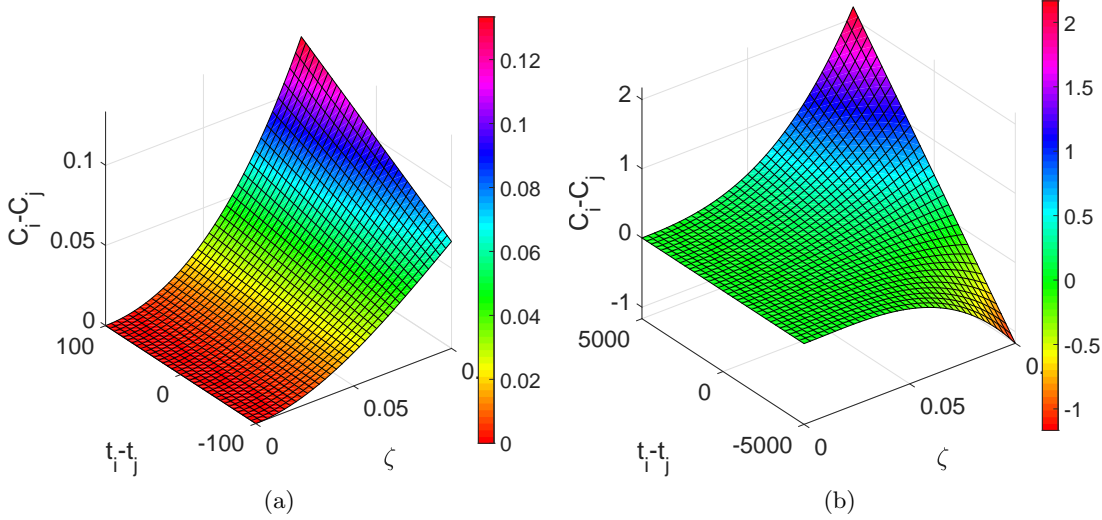


Figure 12: Illustration of the change in the difference in the risk-dependent centrality of nodes having a small difference in degrees, $k_i - k_j = 100$, as a function of the difference in the number of triangles, $-100 \leq \Delta \leq 100$ (a) and $-5000 \leq \Delta \leq 5000$ (b), and of the network infectivity (risk) ζ .

To illustrate how well the estimate (7.6) performs, we use it for approximating the interlacement point for several pairs of corporates and compare them with the observed values in Table 4 for the weighted version of the US corporate network.

Table 4: Calculation of the crossing point of ranking interlacement for several pairs of corporates in the US corporates network of 1999 as well as the observed values at which such interlacements occur.

| Plot | Corporate 1 | Corporate 2 | ζ^* calculated | ζ^* observed |
|------|-------------------------|-------------------------|----------------------|--------------------|
| (a) | J.P. Morgan&Co Inc. | Bank of America Corp. | 0.375 | 0.37 |
| (b) | Pfizer Inc. | Ashland Inc. | 0.441 | 0.41 |
| (c) | Morgan Stanley & Co. | Bank One Corp. | 0.176 | 0.17 |
| (d) | AT&T Corp. | Airtouch Communications | 0.273 | 0.27 |
| (e) | Union Carbide Corp. New | AON Corp. | 0.353 | 0.32 |
| (f) | General Motors Corp. | Boeing Co. | 0.214 | 0.14 |

A few more general considerations on the validity of the power series truncation heuristic can be made. The size of the interval containing any interlacing points is dictated to a large

extent by how quickly the rankings based on the measures $\mathcal{C}_i(\zeta)$ (or $\tilde{\mathcal{C}}_i(\zeta)$) stabilize near the rankings obtained using eigenvector centrality. This, in turn, depends on the spectral gap $\lambda_1 - \lambda_2$: the larger the gap, the faster the eigenvector centrality rankings are approached for increasing values of ζ . Hence, in the case of relatively large gaps, we expect any interlacing values to occur for fairly small values of ζ . In this case, the heuristics based on polynomial approximations may be justified, since interlacing is likely to occur already for small values of ζ . As is well known, however, it is not easy to determine when the spectral gap is “sufficiently large”. On the other hand, when the spectral gap is tiny, then the interval $[0, \bar{\zeta}]$ is going to be larger and therefore there is “more room” for the occurrence of interlacing. Unfortunately, in this case it is not clear that polynomial truncation will be effective in approximately locating the interlacing points. In this case, a possible solution is to expand the functions $\mathcal{C}_i(\zeta)$ not around the value $\zeta = 0$, but also around a few values $\zeta_0 > 0$. This strategy can also be used to find a possible second point of interlacing after having found a first such point ζ^* . Expanding around ζ^* leads to

$$\begin{aligned} \Psi(\zeta^* + \eta) &= \mathcal{C}_i(\zeta^* + \eta) - \mathcal{C}_j(\zeta^* + \eta) = \\ &= \frac{1}{2!}(w_{i,i}^{(2)} - w_{j,j}^{(2)})\eta^2 + \frac{1}{3!}(w_{i,i}^{(3)} - w_{j,j}^{(3)})\eta^3 + \cdots + \frac{1}{k!}(w_{i,i}^{(k)} - w_{j,j}^{(k)})\eta^k + O(\eta^{k+1}). \end{aligned}$$

Dividing by η^2 and setting the result equal to zero leads to an algebraic equation of degree $k-2$ for η ; the smallest positive root η^* of this equation, if there are any, leads to the approximation $\zeta^* + \eta^*$ for the next interlace point, and so forth.

Completely analogous considerations apply to the approximation of interlacing points when the ranking of nodes is done according to the risk-based total communicability measure $\mathcal{R}_i(\zeta)$. In this case the transcendental equation to be solved is given by

$$\chi(\zeta) = \mathcal{R}_i(\zeta) - \mathcal{R}_j(\zeta) = \sum_{k=1}^n e^{\zeta \lambda_k} \left(\psi_k^T \vec{1} \right) [\psi_{k,i} - \psi_{k,j}] = 0.$$

Let $w_i^{(k)} = (A^k \vec{1})_i$. Then, truncating the series expansion (7.1) and dividing by $\zeta > 0$ leads to the approximation

$$(7.7) \quad \frac{(w_i^{(k)} - w_j^{(k)})}{k!} \zeta^{k-1} + \cdots + \frac{(w_i^{(2)} - w_j^{(2)})}{2!} \zeta + (w_{i,i}^{(2)} - w_{j,j}^{(2)}) = 0$$

for the equation whose smallest positive solution approximates the first interlacement value for the rankings of nodes i and j , assuming it exists; here again $k \geq k_0$ where now $k_0 \geq 2$ is the smallest integer value for which the sequence $\{w_i^{(k)} - w_j^{(k)}\}_k$ changes sign. The simplest possible case is when $k = k_0 = 2$, which occurs when $w_{i,i}^{(2)} - w_{j,j}^{(2)}$ and $w_i^{(2)} - w_j^{(2)} = (A^2 \vec{1})_i - (A^2 \vec{1})_j$ have different sign. In this case (7.7) reduces to the linear equation

$$\frac{(w_i^{(2)} - w_j^{(2)})}{2} \zeta + (w_{i,i}^{(2)} - w_{j,j}^{(2)}) = 0,$$

with the unique root

$$\zeta^* = 2 \frac{w_{i,i}^{(2)} - w_{j,j}^{(2)}}{w_j^{(2)} - w_i^{(2)}} > 0.$$

8. Conclusions. In general, node centrality in networks are of either of two types: (i) node centrality in networks of time-invariant topology [41], or (ii) node centrality in networks of time-dependent topology (aka temporal networks) [60]. In this work we have developed a new concept of node centrality, depending on both the topology of the network and the external conditions to which the network as a whole is submitted. In particular, we have focused on global risk as the external factor by which an economic and financial network is affected. We started by considering the “Susceptible-Infected” model and its connection to the communicability functions of nodes and edges in a network. Then, we developed a few centrality measures which depend not only on the local and global topological environment of a node but also on the level of infectivity stressing the system as a whole. In this way we have been able to make predictions in financial and economic systems about the changes in the risk-dependent centralities of nodes as a function of the global level of infectivity in the system. We observe that without altering the topology of the network, i.e., without varying any connection between the nodes, the ranking of the nodes, according to these new centrality measures, changes significantly as the infectivity rate changes. In the real-world networks studied here we have been able to associate those changes in the risk-dependent centrality of nodes with events of the real financial and economic worlds in which these networks are embedded. In closing, we provide here both theoretical, computational and empirical evidences that the node centrality is not a static function even when the topology of the system is not varying at all. This new paradigm is expected to play a fundamental role in assessing the robustness of financial and economic systems to the variation of the external conditions which they are submitted to.

REFERENCES

- [1] D. ACEMOGLU, A. OZDAGLAR AND A. TAHBAZ-SALEHI, *Systemic risk and stability in financial networks*, Am. Econ. Rev., 105(2) (2015), pp. 564-608.
- [2] F. ALLEN AND A. BABUS, *Networks in finance* in The network challenge: strategy, profit and risk in an interlinked world, Wharton School Publishing 2009.
- [3] F. ALLEN AND D. GALE, *Financial Contagion*, J. Political Econ., 108 (2000), pp.1-33.
- [4] R. ALQUIST, R. MUKHERJEE AND L. TESAR, *Fire-sale FDI or Business as Usual?*, Working Paper, National Bureau of Economic Research, 2013.
- [5] I. ALVES, S. FERRARI, P. FRANCHINI, J.C. HEAM, P. JURCA, S. LANGFIELD, S. LAVIOLA, F. LIEDORP, A. SANCHEZ, S. TAVOLARO AND G. VUILLEMEY, *The structure and resilience of the European inter-bank market*, Working Paper, European Systemic Risk Board, 2013.
- [6] H. AMINI, R. CONT AND A. MINCA *Resilience to contagion in financial networks*, Math Financ, 26(2) (2016), pp. 329-65.
- [7] M. BARDOSCIA, S. BATTISTON, F. CACCIOLI AND G. CALDARELLI, *DebtRank: A Microscopic Foundation for Shock Propagation*, PloS One, 10 (2015), pp 1-13.
- [8] M. BARDOSCIA, S. BATTISTON, F. CACCIOLI AND G. CALDARELLI, *Pathways towards instability in financial networks*, Nat. Commun., 8 (2017).
- [9] M. BARDOSCIA, F. CACCIOLI, J. I. PEROTTI, G. VIVALDO AND G. CALDARELLI, *Distress Propagation in Complex Networks: The Case of Non-Linear DebtRank*, PloS One, 11 (2016), pp 1-12.
- [10] S. BATTISTON, G. CALDARELLI, R. M. MAY, T. ROUKNY AND J. E. STIGLITZ, *The price of complexity in financial networks*, Proceedings of the National Academy of Sciences, 113 (36) (2016), pp. 10031-10036.
- [11] S. BATTISTON, D. DELLI GATTI, M. GALLEGATI, B. GREENWALD AND J.E. STIGLITZ, *Liaisons dangereuses: Increasing connectivity, risk sharing, and systemic risk* J. Econ. Dyn. Control, 36(8) (2012),

- pp. 1121-1141.
- [12] S. BATTISTON, D. DELLI GATTI, M. GALLEGATI, B. GREENWALD AND J.E. STIGLITZ, *Default cascades: When does risk diversification increase stability?*, J. Financ. Stabil., 8(3) (2012), pp. 138-149.
 - [13] S. BATTISTON, M. PULIGA, R. KAUSHIK, P. TASCA AND G. CALDARELLI *DebtRank: too central to fail? financial networks, the FED and systemic risk*, Sci. Rep. 2, 541 (2012) pp.1-6.
 - [14] M. BENZI AND P. BOITO, *Quadrature rule-based bounds for functions of adjacency matrices*, Linear Algebra Appl., 433 (2010), pp. 637-652.
 - [15] M. BENZI AND C. F. KLYMKO, *Total communicability as a centrality measure*, J.Complex Netw., 1 (2013), pp. 124-149.
 - [16] M. BENZI AND C. F. KLYMKO, *On the limiting behavior of parameter-dependent network centrality measures*, SIAM J.Matrix Anal.Appl., 36 (2015), pp. 686-706.
 - [17] P. BONGINI, G.P. CLEMENTE AND R. GRASSI, *Interconnectedness, G-SIBs and network dynamics of global banking*, Finance Res Lett, 27 (2018), pp.185-192.
 - [18] M. BOSS, H. ELSINGER, M. SUMMER AND S. THURNER, *An empirical analysis of the network structure of the Austrian Interbank Market*, Financial Stability Report, Oesterreichische National-bank, 2004.
 - [19] F. CACCIOLI, T.A. CATANACH AND J.D. FARMER, *Heterogeneity, correlations and financial contagion*, Adv. Complex Syst. (2012), 15(supp02):1250058.
 - [20] G. CALDARELLI, A. CHESSA, F. PAMMOLLI, A. GABRIELLI AND M. PULIGA, *Reconstructing a credit network*, Nat. Phys., 9 (2013), pp. 125-126.
 - [21] M. CHINAZZI AND G. FAGIOLO, *Systemic risk, contagion, and financial networks: A survey*, Institute of Economics, Scuola Superiore Sant'Anna, Laboratory of Economics and Management (LEM) Working Paper Series. 2015.
 - [22] R. CIFUENTES, G. FERRUCCI AND H.S. SHIN, *Liquidity Risk and Contagion*, J. Eur. Econ. Assoc., 3 (2005), pp. 556-566.
 - [23] G.P. CLEMENTE, R. GRASSI AND C. PEDERZOLI, *Networks and market-based measures of systemic risk: the European banking system in the aftermath of the financial crisis*, J. Econ. Interact. Coord., (2019), pp.1-23.
 - [24] J. COCCO, F. GOMES AND N. MARTINS, *Lending relationships in the interbank market*, J. Financ. Intermed., 18 (1) (2009), pp. 24-48.
 - [25] L. COHEN, A. FRAZZINI AND C. MALLOY, *The small world of investing: Board connections and mutual fund returns*, J. Political Econ., 116(5) (2008), pp. 951-979.
 - [26] M. COROMINAS-BOSCH, *Bargaining in a network of buyers and sellers*, J. Econ. Theory, 115(1) (2004), pp.35-77.
 - [27] T.M. COVER AND J.A. THOMAS, *Elements of Information Theory*, Wiley & Sons, 2006.
 - [28] A. DASGUPTA, *Financial Contagion Through Capital Connections: A Model of the Origin and Spread of Bank Panics*, J. Eur. Econ. Assoc. 2, (2004), pp. 1049-1084.
 - [29] J. DE WEERDT, *Risk-sharing and endogenous network formation*. WIDER Discussion Papers, World Institute for Development Economics (UNU-WIDER), 2002.
 - [30] N. DEMIRIS, T. KYPRAIOS AND L.V. SMITH, *On the epidemic of financial crises*, J R Stat Soc Ser A Stat Soc, 177(3), (2014), pp. 697-723.
 - [31] N. DETERING, T. MEYER-BRANDIS, K. PANAGIOTOU, AND D. RITTER, *Managing default contagion in inhomogeneous financial networks*, SIAM J. Finan. Math., 10(2), (2019) pp.578-614.
 - [32] K. DIMITRIOS AND O. VASILEIOS, *A network analysis of the Greek stock market*, Procedia Econ. Financ, 33 (2015) 340-9.
 - [33] J.C. DUAN, AND C. ZHANG, *Cascading defaults and systemic risk of a banking network*, NUS Working Paper, 2013.
 - [34] N. ECONOMIDES, *The economics of networks*, Int. J. Ind. Organ., 14(6) (1996), pp. 673-99.
 - [35] S. EDWARDS, *Capital flows and the emerging economies: Theory, evidence, and controversies*, National Bureau of Economic Research Book, University of Chicago Press, 2008.
 - [36] L. EISENBERG, AND T. NOE, *Systemic risk in financial systems*, Manage. Sci., 47 (2001), pp.236-249.
 - [37] M. ELLIOTT, B. GOLUB AND M. O. JACKSON, *Financial Networks and Contagion*, Am. Econ. Rev., 104(10) (2014), 3115-3153.
 - [38] H. ELSINGER, A. LEHAR AND M. SUMMER, *Using market information for banking systems*, Int. J. Central Bank., 27 (2006), pp. 137-165.

- [39] P. ERDŐS AND A. RNYI, *On the evolution of random graphs*, Publ. Math. Inst. Hungar. Acad. Sci., 5 (1960), pp.17-61.
- [40] P. ERDŐS AND A. RNYI, *On the strength of connectedness of a random graph*, Acta Math. Hung., 12(1-2) (1961), pp. 261-267.
- [41] E. ESTRADA, *The structure of complex networks: theory and applications*, Oxford University Press, 2012.
- [42] E. ESTRADA AND N. HATANO, *Communicability in complex networks*, Phys. Rev. E., 77(3) (2008).
- [43] E. ESTRADA AND N. HATANO, *A vibrational approach to node centrality and vulnerability in complex networks*, Physica A Stat. Mech. Appl., 389(17),(2010) pp. 3648-3660.
- [44] E. ESTRADA, J.A. RODRIGUEZ-VELZQUEZ, *Subgraph centrality in complex networks*, Phys. Rev. E, 71 (2005).
- [45] M. FAFCHAMPS AND F. GUBERT, *The formation of risk sharing networks*, J. Dev. Econ., 83(2) (2007), pp. 326-350.
- [46] M. FAFCHAMPS AND S. LUND, *Risk-sharing networks in rural Philippines*, J. Dev. Econ., 71(2) (2003), pp.261-287.
- [47] J. FOSTER, *From simplistic to complex systems in economics*, Camb. J. Econ., 29 (2005) pp. 873-892.
- [48] X. FREIXAS, B. PARIGI AND J.C. ROCHET, *Systemic risk, interbank relations and liquidity provision by the central bank* J. Money Credit Bank. 32, (2000), pp. 611-638.
- [49] T. FURUSAWA AND H. KONISHI, *Free trade networks*, J. Int. Econ., 72(2) (2007), pp.310-35.
- [50] P. GAI, A.G. HALDANE AND S. KAPADIA, *Complexity, concentration and contagion*, J.Monetary Econ., 58 (5) (2011), pp.453-470.
- [51] P. GAI AND S. KAPADIA, *Contagion in Financial Networks*, Proc. Royal Soc. A, 466 (2010), pp. 2401-23.
- [52] D.M. GALE AND S. KARIV, *Financial networks*. Am. Econ. Rev., 97(2) (2007), pp. 99-103.
- [53] A. GALEOTTI AND S. GOYAL, *A theory of strategic diffusion*, Working Paper 2007.
- [54] P. GIUDICI, P. SARLIN AND A. SPELTA, *The interconnected nature of financial systems: direct and common exposures*, J. Bank. Finance, (2017).
- [55] P. GLASSERMAN AND H.P. YOUNG *How likely is contagion in financial networks?*, J. Bank. Finance, 50 (2015) pp. 383-99.
- [56] R. GLICK AND A. ROSE, *Contagion and trade: Why are currency crises regional?*, J. Int. Money Finance, 18(4) (1999), pp. 603-617.
- [57] B. GOLUB AND M.O. JACKSON, *Naive learning in social networks: Convergence, influence, and the wisdom of crowds*, preprint 2007, available online from <http://www.people.fas.harvard.edu/~bgolub/papers/naivelearning.pdf>.
- [58] S. GOYAL AND J.L. MORAGA-GONZALEZ, *R&D networks*, Rand J. Econ., 1 (2001), pp.686-707.
- [59] A.G. HALDANE AND R.M. MAY, *Systemic Risk in Banking Ecosystems*, Nature, 469 (2011), pp. 351-355.
- [60] P. HOLME AND J. SARMAKI, *Temporal networks*, Physics Reports, 519 (3) (2012), pp. 97-125.
- [61] X. JIA AND R. TOMASIC, *Corporate governance and resource security in China: The transformation of China's global resources companies*, 1st ed., Routledge Studies in Corporate Governance, CRC Press, 2015.
- [62] M. KANNO, *Assessing systemic risk using interbank exposures in the global banking system*, J. Financ. Stabil., 20C (2015), pp.105-130.
- [63] L. KATZ, *A new status index derived from sociometric data analysis*, Psychometrika, 18 (1953), pp. 39-43.
- [64] M.L. KATZ AND C. SHAPIRO, *Systems competition and network effects*, J. Econ. Perspect., 8(2) (1994), pp. 93-115.
- [65] A. KIRMAN, *The economy as an evolving network*, J. Evol. Econ., 7(4) (1997), pp.339-53.
- [66] K. KLOSTER, Talk delivered at the International Conference on Industrial and Applied Mathematics (ICIAM 2019), Valencia, Spain, July 16, 2019, and personal communication.
- [67] Y. KORNIYENKO, M. PATNAM, R. M. DEL RIO-CHANONA AND M. A. PORTER, *Evolution of the Global Financial Network and Contagion: a New Approach*, IMF Working Paper, 2018.
- [68] O. KOSTYLENKO, H.S. RODRIGUES AND D.F.M. TORRES, *The spread of a financial virus through Europe and beyond*, AIMS Math., 4(1) (2019), pp.86-98.
- [69] F. KRAMARZ AND D. THESMAR D., *Social networks in the boardroom*, J. Eur. Econ. Assoc., 11(4) (2013), pp.780-807.
- [70] R.E. KRANTON AND D.F. MINEHART D.F., *A theory of buyer-seller networks*, Am. Econ. Rev., 91(3) (2001), pp.485-508.

- [71] W. LAZONICK AND E. MARCH, *The rise and demise of Lucent Technologies*, Working Paper, Munich Personal RePEc Archive, 2010.
- [72] C.H. LEE, S. TENNETI AND D.Y. EUN, *Transient Dynamics of Epidemic Spreading and its Mitigation on Large Networks*, ArXiv preprint arXiv:1903.00167, 2019.
- [73] K.M. LEE, J.S. YANG, G. KIM, J. LEE, K.I. GOH AND I. M. KIM, *Impact of the Topology of Global Macroeconomic Network on the Spreading of Economic Crises*, PLoS One, 6(3) (2011) e18443.
- [74] Y. LEITNER, *Financial Networks: Contagion, Commitment, and Private Sector Bailouts*, J. Finance 60, (2005), 2925-2953.
- [75] D. LPEZ-PINTADO, *Diffusion in complex social networks*, Games Econ. Behav., 62(2) (2008), pp.573-590.
- [76] R.N. MANTEGNA, *Hierarchical structure in financial markets*. Eur. Phys. J. B., 11(1) (1999), pp. 193-197.
- [77] R. M. MAY, S.A. LEVIN AND G. SUGIHARA, *Complex systems: ecology for bankers*, Nature, 451 (2008), 893-895.
- [78] W. MEI, S. MOHAGHEGHI, S. ZAMPIERI AND F. BULLO, *On the dynamics of deterministic epidemic propagation over networks*, Annual Reviews in Control, 44, (2017), pp. 116-128.
- [79] C. MINOIU AND J.A. REYES, *A network analysis of global banking: 1978-2010*, J Financ. Stabil., 9(2) (2013), pp. 168-184.
- [80] M.E. NEWMAN, *A measure of betweenness centrality based on random walks*, Soc. Netw., 27(1) (2005), pp. 39-54.
- [81] B. NGUYEN-DANG, *Does the rolodex matter. Corporate Elite's Small World and the Effectiveness of Boards of Directors*, SSRN Working Paper, 2007.
- [82] C. NOWZARI, V. M. PRECIADO AND G. J. PAPPAS *Analysis and control of epidemics: A survey of spreading processes on complex networks*, IEEE Contr. Syst. Mag., (2016) pp. 26-46
- [83] J.P. ONNELA, A. CHAKRABORTI, K KASKI, J. KERTSZ AND A. KANTO, *Dynamics of market correlations: Taxonomy and portfolio analysis*, Phys. Rev. E, 68(5) (2003).
- [84] J.P. ONNELA, J. SARANKI, J. KERTSZ AND K.KASKI, *Intensity and coherence of motifs in weighted complex networks*, Phys. Rev. E., 71(6) (2005).
- [85] R. PASTOR-SATORRAS, C. CASTELLANO, P. VAN MIEGHEM AND A. VESPIGNANI, *Epidemic processes in complex networks*, Rev. Mod. Phys., 87(3) (2015).
- [86] G. PERALTA AND A. ZAREEI, *A network approach to portfolio selection*, J. Empir. Finance, 38 (2016), pp. 157-180.
- [87] F. POZZI, T. DI MATTEO AND T. ASTE, *Spread of risk across financial markets: better to invest in the peripheries*, Scientific reports, 2013.
- [88] C. PUHR, R. SELIGER AND M. SIGMUND, *Contagiousness and vulnerability in the Austrian interbank market*, Financial Stability Report 24, Oesterreichische National-bank, 2012.
- [89] A. SACHS, *Completeness, interconnectedness and distribution of interbank exposures? a parameterized analysis of the stability of financial networks*, Quant. Financ., 14(9) (2014), pp. 1677-1692.
- [90] B.M. TABAK, M. TAKAMI, J.M.C. ROCHA, D.O. CAJUEIRO AND S.R.S. SOUZA, *Directed clustering coefficient as a measure of systemic risk in complex banking networks*, Physica A, 394 (2014), pp.211-216.
- [91] M. TIRADO, *Complex network for a crisis contagion on an international system*, Int. J. Modern Phys. C, 23(9) (2012).
- [92] M. TOIVANEN, *Contagion in the interbank network: An epidemiological approach*, Bank of Finland Research Discussion Paper, 2013.
- [93] C. UPPER, *Simulation methods to assess the danger of contagion in interbank markets*, J Financ Stabil, 7(3) (2011), pp. 111-125.
- [94] P. VAN MIEGHEM, K. DEVRIENDT AND H. CETINAY, *Pseudoinverse of the Laplacian and best spreader node in a network*, Phys. Rev. E., 96 (2017).
- [95] P. VAN MIEGHEM, J. OMIC AND R. KOOLJ, *Virus Spread in Networks*, IEEE ACM T NETWORK, 17(1) (2009).
- [96] S. VIVIER-LIRIMONT, *Interbanking networks: towards a small financial world?*, Working Paper Universit Panthon-Sorbonne (Paris 1), 2004.